MATHEMATICAL MODELING OF SHADING BY OBSTACLES AND PREDICTION OF OPTIMAL ENERGY GENERATION FROM A SOLAR PV SYSTEM PER UNIT AREA OVER THE YEAR

A thesis submitted in partial fulfillment of the

requirements for the degree of Master of Science

in Renewable Energy Technology

Institute of Energy, University of Dhaka

By

Shah Mohammad Mohiuddin Siddique

Examination Roll number: 527

Registration number: Ha-299

Admission session: 2013 - 2014

September 2016

Supervisor's Declaration

The MS level research on "Mathematical modeling of shading by obstacles and prediction of optimal energy generation from a solar PV system per unit area over the year" has been carried out and the dissertation was prepared under my direct supervision. Hereby I confirm that, to the best of my knowledge the thesis represents the original research work of the candidate; the contribution made to the research by me, by others of the University was consistent with normal supervisory practice, and external contributions to the research are acknowledged.

I believe the thesis to be in a suitable presentational form and is ready for examination.

Date: ____________________

Dr. Himangshu Ranjan Ghosh
Lecturer
Institute of Energy, University of Dhaka
Dhaka, Bangladesh

Candidate's Declaration

I confirm that this thesis represents my own work; the contribution of any supervisors and others to the research and to the thesis was consistent with normal supervisory practice. External contributions to the research are acknowledged.

Date: ____________________

Shah Mohammad Mohiuddin Siddique
MS student
3rd Semester, Admission Session 2013-2014
Institute of Energy, University of Dhaka
Dhaka, Bangladesh

Dedicated to –

To my little brother, Shah Mohammad Ahasan Siddique

My parents who always strengthen and encourage me to sail across.

Acknowledgement

This work was carried out at the Institute of Energy at University of Dhaka, Bangladesh during the years 2015-2016. I want to thank Dr. Himangshu Ranjan Ghosh for supervising my thesis and encouraging me throughout my efforts towards the Master degree. And I thank the Director, Dr. Saiful Haque and all other teachers who taught us about many things during the course. I also thank all the staffs In the Institute of Energy, University of Dhaka who provided a productive and inspiring working environment.

I also thank my parents for encouraging me during my work and studies.

Abstract

There is an exponential growth and growing popularity of solar photovoltaic technology for energy generation in comparison with the conventional and other renewable energy sources. But the massive utilization of this technology is hindered by space constraints. And that is why optimal use of space with solar PV modules is a pre-requisite for optimal energy generation per unit area. In this research, the sun-path diagram, surrounding obstacles shading, optimal PV module row spacing have been analyzed and a mathematical model have been developed which is solved using Mat lab. This study shows that the optimal module row spacing is about 1 meter considering comparatively effective sunshine hour (9:00am to 3:00pm) for commercial systems. The minimum module row spacing calculated from sun-path diagram is about 1 meter under the same condition. Deviation between the values of module row spacing calculated from these two method is only 1.05%. Power generation per unit area by minimum module row spacing calculated from our proposed model is about 250 kWh per square meter land area. Return rate of money due to the use of minimum row spacing is about 20%. Moreover in this research a shading diagram has been proposed to study the effect of obstacles over the year on a solar system drawn by the overlaying of horizontal-profile over sun-path diagram which will provide information about which obstacles may cause shading at a specific time of day and year. It can be analyzed from the shading diagram that which obstacle may affect by shading at specific time over the year. The mathematical model is solved by Mat lab.

Table of Contents

List of Tables

List of Figures

LIST OF ABBREVIATIONS

STC	Standard Test Condition
PV	Photo Voltaic System
PVPS	Photovoltaic Power Systems Program
BPDB	Bangladesh Power Development Board
IDCOL	Infrastructure Development Company Limited
ASTM	American Society for Testing and Materials
IEA	International Energy Agency
AM0	Air Mass Zero
AM 1.5	Air MASS 1.5
NREL	National Renewable Energy Laboratory

LIST OF SYMBOLS

a-Si	Amorphous silicon
CdTe	Cadmium Telluride
CIGS	Copper Indium Gallium Selenide
CO_2	Carbon Dioxide
GaAs	Gallium Arsenide
GaInNAs	Gallium Indium Nitride Arsenide
GaInP	Gallium Indium Phosphide
H_2O	Water
I_0	Dark Saturation Current
I_{01}	Dark Saturation Current in quasi-neutral regions
I_{02}	Dark Saturation Current in depletion region
I_{ph}	Light-generated current
I_{sc}	Short-circuit current
InGaAs	Indium Gallium Arsenide
InGaP	Indium Gallium Phosphide
IEA	International Energy Agency
K	Boltzmann Constant
L_{st}	Standard Meridian (Longitude)
L_{loc}	Local Time
NREL	National Renewable Energy
PV	Photo Voltaic System
q	Elementary Charge
R_s	Series Resistance
R_{sh}	Shunt Resistance
T	Temperature of a PV cell/module
V	Voltage
V_d	Voltage of the diode in one-diode model
V_t	Thermal Voltage

CHAPTER 1
INTRODUCTION

1. Introduction

The increasing of human population is putting an incremental strain on fossil fuel energy resources. And the present world's economy depends on fossil fuel. Fossil fuels are an incredibly dense form of energy, and they took millions of years to become so. And when they're gone, they're gone pretty much forever. It's only a matter of time. Globally - every year we currently consume the equivalent of over 11 billion tons of oil in fossil fuels. Crude oil reserves are vanishing at the rate of 4 billion tons a year. [1]. If we carry on at this rate without any increase for our growing population or aspirations, our known oil deposits will be gone by 2052.

We'll still have gas left, and coal too. But if we increase gas production to fill the energy gap left by oil, then those reserves will only give us an additional eight years, taking us to 2060. But the rate at which the world consumes fossil fuels is not standing still, it is increasing as the world's population increases and as living standards rise in parts of the world that until recently had consumed very little energy. Fossil Fuels will therefore run out earlier.

It's often claimed that we have enough coal to last hundreds of years. But if we step up production to fill the gap left through depleting our oil and gas reserves, the coal deposits we know about will only give us enough energy to take us as far as 2088. And let's not even think of the carbon dioxide emissions from burning all that coal.

Graph showing future energy reserves for coal, gas and oil.

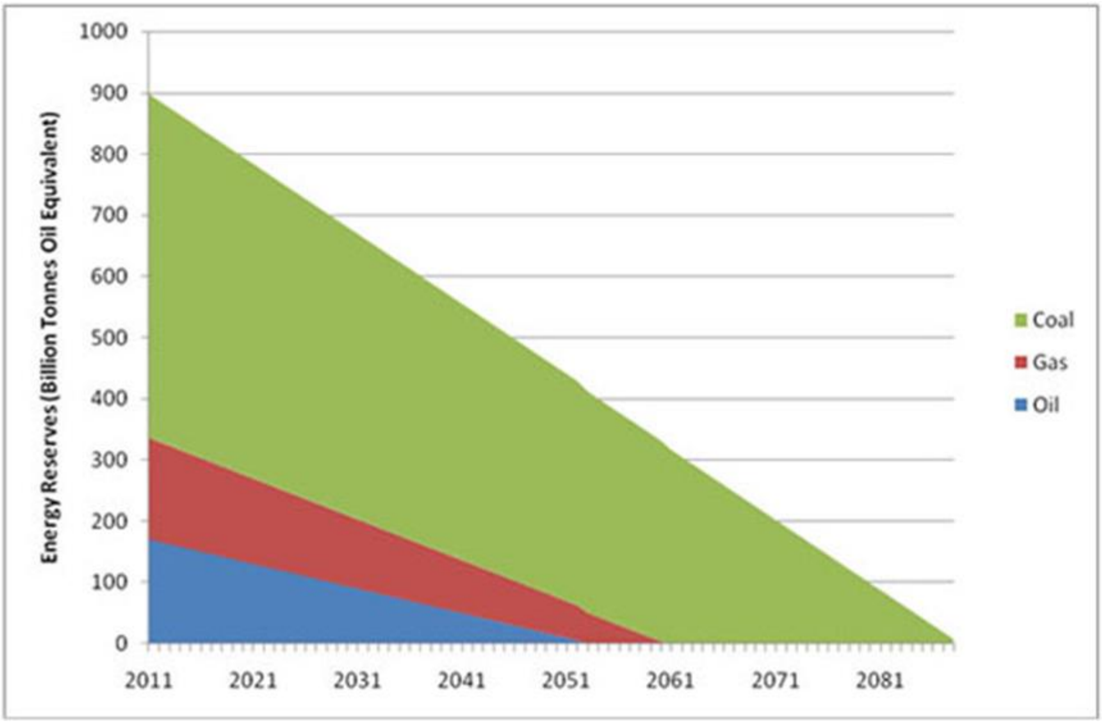

Figure 1-1: Possible usage of different fossil fuels in future and their probable ending time. [1]

In the diagram, we can see that year 2088 is marking the end of fossil fuel reserves. But that’s not what is going to happen. Some new reserves will be found which will help extend this deadline slightly, but these can’t last forever. New reserves of fossil fuels are becoming harder to find, and those that are being discovered are significantly smaller than the ones that have been found in the past.

If we take oil, for example, we’re probably already on a downward slope. Sixteen of the world’s twenty largest oil fields have already reached their peak level of production (the point at which they are producing their largest annual oil yield), whilst the golden age of oil field discovery was nearly 50 years ago.

Renewables offer us another way, a way to avoid this (fossil fueled) energy time bomb, but we must we start now. As the Saudi Oil Minister said in the 1970s, “The Stone Age didn’t end for lack of stone, and the oil age will end long before the world runs out of oil.”[1]

So due to this the world leading economically developed countries started to research on renewable energy sources which won’t be finished till to the end of the world.

Renewable energy is generally defined as energy that comes from resources that are not significantly depleted by their use, such as sunlight, wind, rain, tides, waves and geothermal heat. [2] Renewable energy is gradually replacing conventional fuels in four distinct areas: electricity generation, hot water/space heating, motor fuels, and rural (off-grid) energy services. [3]

Based on REN21's 2016 report, renewables contributed 19.2% to humans' global energy consumption and 23.7% to their generation of electricity in 2014 and 2015, respectively. This energy consumption is divided as 8.9% coming from traditional biomass, 4.2% as heat energy (modern biomass, geothermal and solar heat), 3.9% hydro-electricity and 2.2% is electricity from wind, solar, geothermal, and biomass. Worldwide investments in renewable technologies amounted to more than US$286 billion in 2015, with countries like China and the United States heavily investing in wind, hydro, solar and biofuels. [4]

Globally, there are an estimated 7.7 million jobs associated with the renewable energy industries, with solar photovoltaics being the largest renewable employer. [5]

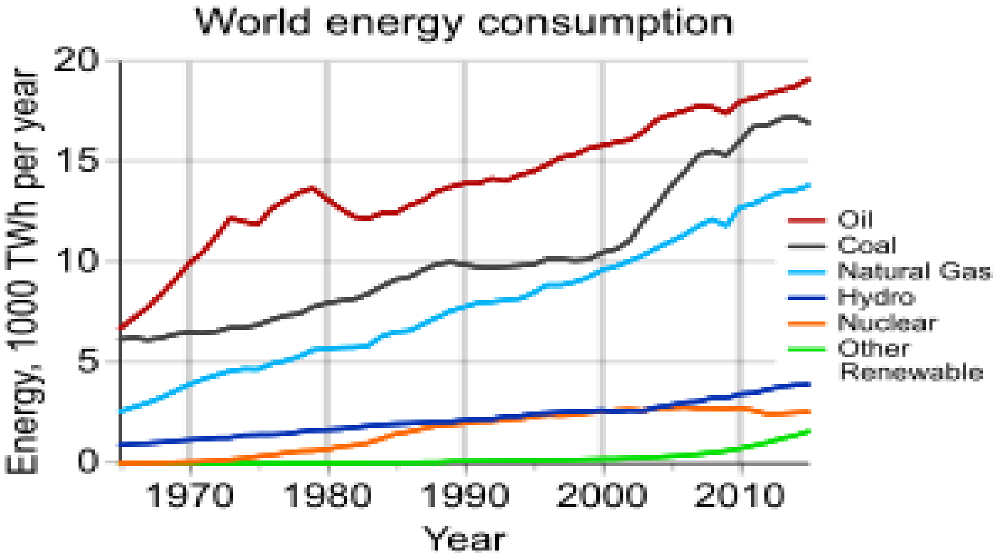

Figure - 1.2: The world's increasing demand for energy. [6]

It's clearly seen from the data and the world energy consumption there is a rapid development in the field of power generation from renewable energy. And Solar photovoltaics is one of the important renewable energy technology.

The energy of solar radiation is vital to all living species on out planet and the amount of energy is substantial. The amount of energy coming from the sun to earth in one hour is more than the mankind consumes in a year. [7]

There is a tremendous potential to provide the entire world's energy needs by simply harnessing power from the sun. A photovoltaic (PV) system directly converts light to electricity and is a cost-efficient and sustainable method of energy production for a long term investment. PV power is widely used throughout the whole world in various formats like Photovoltaic Power Plant (fixed type or single or double axes Sun tracker type), Isolated Grid type, Photovoltaic Mini Grid type, backup power system for a multistoried building, or household buildings and etc. From Bangladesh perspective, all the PV modules are needed to import from the manufacturing countries; till today at our maximum level of technical competency we can just assemble the imported solar cells here, but the efficiency becomes a bit less than usually imported one. Though we can get a PV module with a cheaper price, we have to use its maximum areas and capacity under solar irradiation.

Preliminary reported market data shows a growing market in 2015. At least 48.1 GW of PV systems have been installed and connected to the grid in the world last year. While these data will have to be confirmed in the coming months, some important trends can already be discerned:

------The global PV market grew significantly, to at least 48.1 GW in 2015. With non-reporting countries, this number could grow up to 50 GW, compared to 40 GW in 2014. This represents a 25% growth year on. The 2 GW comprise non IEA PVPS markets countries such as Pakistan, Uruguay, Brazil, Guatemala and more.

------Asia ranks in first place for the third year in a row with around 60% of the global PV market.

-------China reached 15.3 GW in 2015, and is now the leader in terms of cumulative capacity with 43.6 GW.

-------Japan continued to grow slightly with around 11 GW installed and connected to the grid in 2015.

-------The market in Europe has progressed for the first time in years from 7 GW in 2014 to around 8 GW in 2015.

-------The US market increased again to 7.3 GW, with large scale and third party ownership dominating.

-------Several established markets confirmed their maturity in 2015, including Korea (1.0 GW), Australia (0.9 GW), Canada (0.6 GW), Taiwan (0.4 GW est.) and more.

-------India progressed significantly to around 2 GW and Pakistan installed an estimated 600 MW.

-------Emerging markets continued to contribute to the global PV development in 2015:

South Africa (200 MW), Chile (446 MW), Mexico (103 MW), Turkey (208 MW), Honduras (389 MW), the Philippines (122 MW), Algeria (268 MW) and more.

-------The MEA markets experienced growth, thanks to South Africa, Algeria, Israel and Turkey.

-------The largest European market in 2015 was UK with 3.51 GW, followed by Germany (1.46 GW) and a stable French market (0.87 GW).

-------In the top 10 countries, there are 5 Asia Pacific countries (China, Japan, India, Korea and Australia), three European countries (UK, Germany and France) and two countries in the North American region (USA, Canada).

-------The level to enter the top 10 in 2015 was around 600 MW.

-------Italy, Greece and Germany now have enough PV capacity to produce respectively 8%, 7.4% and 7.1% of their annual electricity demand with PV. 22 countries have enough PV capacity to produce at least 1% of their electricity demand with PV.

--------PV represents at least 3,5% of the electricity demand in Europe and 7% of the peak electricity demand.

--------PV represents around 1.3% of the global electricity demand.

--------23 countries had at least 1 GW of cumulative PV systems capacity at the end of 2015 (2 reached that level in 2015) and 7 countries installed at least 1 GW in 2015 (compared to 9 in 2013 and 5 in 2014) [8]

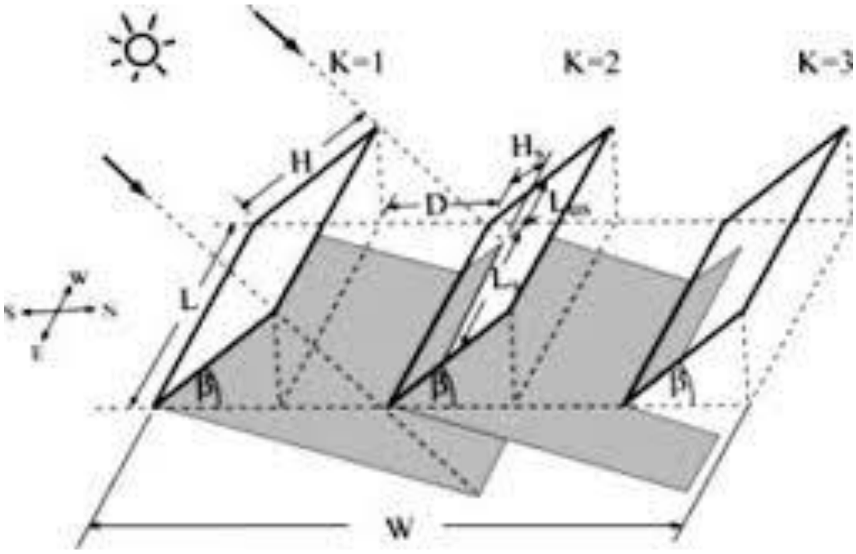

Figure – 1.3: Typical arrangement of Solar PV module of row to row arrangement.

The design of solar power systems (photovoltaic or thermal) of different kinds is increasing and the shading effect of neighboring Photo-Voltaic modules becomes critical for the optimal design of such systems whether it's installed on rooftop or in open space or somewhere else. The shading of Photo Voltaic Panels by their neighbors is likely to occur during some period of the day, especially near Sunrise and Sunset. It is desired that any shadow be minimized throughout the day. The shading effect depends on the spacing between Photo Voltaic Panels, the row length, their height, the tilt angel, the latitude, the type of Photo Voltaic Panels and the time of year.

The most common and vulnerable shading on row to row arranged PV system is seen like Figure-1.3. Besides panel to panel shading, minor shading form surrounding objects still drastically reduce the performance of a solar cell module. Therefore shade analysis should be performed before installation in order to assess the financial viability of an investment as well as to optimize the location and orientation of a photovoltaic module. [9]

In this work we discuss mathematical formulation of shading effect depending on Sun position in different season also with Sun hour, measuring shadow length and module row spacing variation depending on days of the year for different hour angles, Finally we have suggested the minimum distance between two adjacent rows of PV arrays for avoiding shading effect based on latitude of Dhaka, Bangladesh which is chosen from the hourly shadow length and module row spacing data over the year. We have also devise a mathematical model to find out the minimum shadow length and module row spacing from the sun path diagram of Dhaka city, Bangladesh and we have compare these values with that of the mathematical formulation of shading effect depending on sun position in different seasons also with sun hour. And we have seen that there is a deviation of only about 1% between these two method.

Now taking into the consideration of the value of optimal PV module row spacing from the sun-path diagram, we have calculated optimal electricity generation per square meter, and thus potential return of specific percentage of money.

And finally, from the surrounding environment at the site of Institute of Energy, Dhaka University, we created a horizon profile, showing the elevation of each surrounding object at its specific azimuth angle. Overlaying the horizon profile with the sun path diagram produce a shading diagram, where possible sources of near-object shading is analyzed.

1.1 Motivation of Work

Photovoltaic Cells are the widely used as the source of renewable energy among the other sources like Wind, Hydro, Biomass, Ocean, Tidal, Geothermal and etc. Solar PV system is used widely and extensively due to its availability, portability, module typed; it is also easier to install and also cheaper compared to other source of renewable power system in a small or medium scale of power generation. Eventually solar PV system gives people a great comfort with a comparatively lower investment and minimum lead time for installation and commissioning. Above all the issues Sun is available in every locality with almost same intensity and smaller variation of incidence power due to few parameters like season, geographical location and angle of incidence; and the efficiency is not bad; in 2013, theoretical efficiency has found up to 22.9% [10]. 80 years after 1950 the solar cell efficiency has reached a significant percentage and hopefully the efficiency will be increased.

Over the past decade, since the Bangladesh government launched a rural electrification program supported by the World Bank and other international aid bodies, the number of off-grid installations in the country has rocketed. In 2002, installations rated stood at 7000; today that figure has exploded to nearly 2 million and counting, with average installation rates now topping (approx.) 80,000 a month. [11] So, Bangladesh is the country where a lot of solar panels are used to generated power from the sun.

Bangladesh is a country of small land area with dense population everywhere. Installing Solar PV modules with an effective and efficient way is a great problem due to space limitation. The demand of solar PV system increases so rapidly that no one gets time to calculate a minimum distance between two adjacent rows of solar PV panels regardless any time and season and latitude angle in Bangladesh. Many organizations and personnel are working directly or indirectly in this sector, but when they install the adjacent PV arrays they use their previous experience or take references from theirs mentors to fix the distance between two rows. Eventually, in many cases it has found that partial areas of solar PV panels are shaded by adjacent row in specific time of the day or specific day of a month due to change of season.

The Array IV-curve and PV-curve in case of partial shading is found out by D.B.N. Nandi (2012) and T. Mishima Et al. (2004) is shown are shown as Figure-1.3: [12] [13]

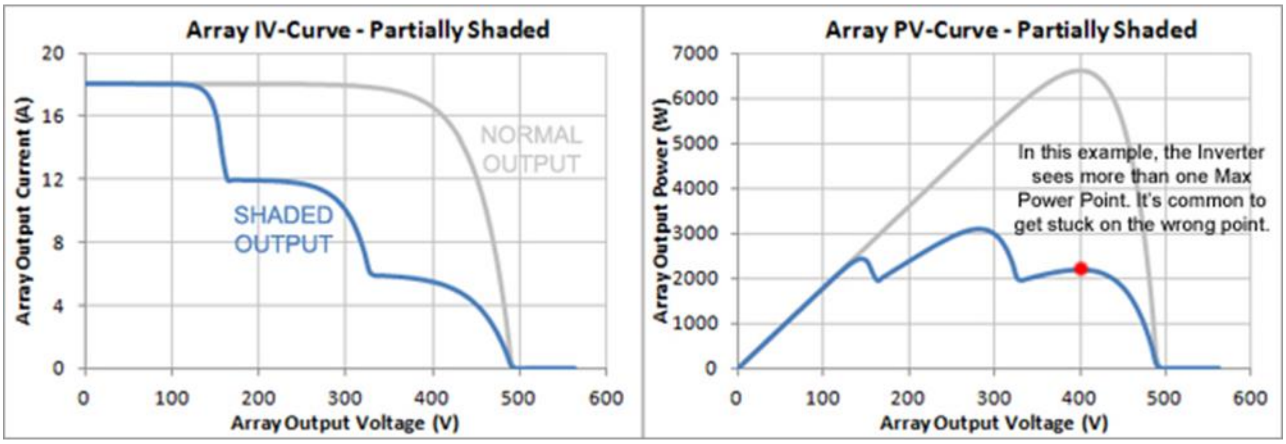

Figure-1.4: I-V (a) and P-V (b) curves of normal and partially shaded series arrays.

The above curve in figure – 3(a) shows that the current gain from a solar PV module under a shaded condition is significantly lower than under normal condition. And in figure-3(b) the power output in shaded condition is also significantly lower than a normal condition of power output from a solar PV module of array.

A study has revealed that the output of a 1400W string – which was fitted with bypass diodes – dropped by 10% when only 4 cells were shaded. When 12 cells were shaded, the power dropped by more than 50%! (R. E. Hanitsch et al., 2001). [14]

If we can't use the solar cells by its maximum capacity, we'll be looser in so many ways – the panels will be inefficient prior to its expected life span, the expected maximum power output will never be received even having a sufficient solar irradiance. We have to invest more money to buy a new set of solar PV modules, eventually our per unit energy generation cost will be higher, which is usually high for a better performed PV system.

More or less we all are well known about the effect of shadows on solar PV panel; but we don't have any concrete data for maintaining minimum distance between row to row during installation of solar PV modules on roof top or open space or somewhere else focusing avoiding shading effect on PV panels. This thesis work tries to say the effects of shading on solar panels and calculate minimum distance between two adjacent rows regardless any latitude angle in anywhere in the world. And thus optimal electricity generation per square meter, and thus potential return of specific percentage of money is also calculated which will give the investor an idea of financial benefit even before the establishment of the panel.

And finally, from the surrounding environment at the site of Institute of Energy, Dhaka University, we created a horizon profile, showing the elevation of each surrounding object at its specific azimuth angle. Overlaying the horizon profile with the sun path diagram produce a shading diagram, where possible sources of near-object shading is analyzed. So the installer will understand that which objects have to be removed before installation and which objects won't give that much shading that can cost minimum electricity generation.

The lesser shading possibility the higher possibility of getting maximum power from PV module, if other installation criteria properly followed.

1.2 Organization of The Thesis

The rest of the thesis is organized as follows

Chapter 2 guides the reader through the amount of energy sun radiate towards the earth and also backgrounds of electrical energy production using PV power generators. Characteristics of solar radiation and the fundamentals of the operation of PV cells will be shortly presented as well as the most important operating conditions on PV cells. Then the basic terminologies, theories explanation to the related work (e.g. declination, angle of incidence, hour angle, azimuth angle, zenith angel, day length, few mathematical explanations and etc.

Chapter 3 focuses on the methodology of how we approach for getting hourly shadow length between two adjacent rows to get maximum power in every day in the year by formulating a mathematical model. Here we have also calculated the Solar azimuth angles and solar altitude angle.

Chapter 4 explains the effect of varying solar geometric parameters on other geometric parameters. The variations and the effects are tabulated and the related graphs are shown for a better understanding. Chronologically the variation of shadow length for inclined PV module for three different tilt angles have tabulated and the related curves are extrapolated. This chapter is simulation works based on matlab and a simple tool to get the minimum distance between two adjacent rows to operate the PV arrays for the year with minimum shading effect.

Chapter 5 focuses on the methodology for finding optimal shadow length for which we can find out a minimum module row spacing and as a result production of energy per square meter will be comparatively more.

Chapter 6 focuses on the methodology for modeling and drawing a sun-path diagram from which we can find out azimuth correction. And by using that azimuth correction we found minimum module row spacing. And we also compare between the minimum module row spacing calculated from the mathematical modeling and also that of the modeling of sun-path diagram.

Chapter 7 focuses on the methodology for obtaining maximum power generation per unit area by using minimum module row spacing. We also calculated power generation per unit area from that of the conventional and we compare between these two. We also calculated the return of money from both the cases and do a comparative study between these two.

Chapter 8 focuses on the methodology of analyzing partial shading of surrounding objects from sun-path diagram. And we also discussed how an investor and installer can decide which obstacles have to be removed and how other obstacles will affect the power generation due to shading over the year.

Finally in conclusion, we have discussed about the result we have found out over the analysis and also discussed what further work can be done on this field.

CHAPTER TWO

BACKGROUND OF THE THESIS

2. Background of The Thesis

This chapter guides the reader through the backgrounds of the stage of the energy of solar radiation by using Photovoltaic Cells. Then discuss in short the effects of shading on PV modules. At first a brief introduction of the characteristics of solar radiation and then the photovoltaic effect and fundamentals of the operation of PV cells is given without diving too deep into semiconductor physics. Then the relevant terminologies of this thesis work and the mathematical explanation for calculating some parameters (e.g. declination angle, hour angle, local time solar time etc.) and al last a brief discussion on shading is explained.

2.1 The Sun As An Energy Resource

The sun is the source of the life on our planet Earth and, directly or indirectly, is the fuel for most renewable systems. Photovoltaic and solar thermal systems, as well as solar thermal power stations, convert solar irradiation directly into useable energy. Continuing our Fundamentals series, Volker Quashing gives an overview of the solar energy resource.

The sun is made up of about 80% hydrogen, 20% helium and only 0.1% other elements. Its radiant power comes from nuclear fusion processes, during which the sun loses 4.3 million tons of mass each second. This mass is converted into radiant energy. Each square meter of the sun's surface emits a radiant power of 63.1 MW, which means that just a fifth of a square kilometer of the sun's surface emits an amount of energy equal to the global primary energy demand on earth. Fortunately, only a small part of this energy reaches the earth's surface. Solar irradiance decreases with the square of the distance to the sun. Since the distance of the earth to the sun changes during the year, solar irradiance outside the earth's atmosphere also varies between 1325 W/m^2 and 1420 W/m^2. The annual mean solar irradiance is known as the solar constant and is 1367±2 W/m^2. On Mars, which is further from the sun than Earth, solar irradiance is below 600 W/m^2 – a factor to be considered when designing PV-powered satellites for the Mars orbit. Only a surface that is perpendicular to the incoming sun's rays receives this level of irradiance. Outside the atmosphere, and therefore not subject to its influence, solar irradiance has only a direct component – all solar radiation is virtually parallel. This irradiance is also called direct normal or beam irradiance. Under these conditions, a surface that is oriented parallel to the sun's rays receives no irradiance. [15]

Various different terms are used when dealing with solar radiation. However, these terms are often used incorrectly, even by some solar specialists. The total specific radiant power, or radiant flux, per area that reaches a Spectrum AM 0 (extraterrestrial) Spectrum AM 1.5 (terrestrial) receiver surface is called irradiance. Irradiance is measured in W/m² and has the symbol E. When integrating the irradiance over a certain time period it becomes solar irradiation. Irradiation is measured in either J/m² or Wh/m², and represented by the symbol H. For daylighting purposes, only the visible part of the sunlight is considered. The analogous quantity to the irradiance for visible light is the illuminance. This uses the unit lm/m² (lumen/m²) or lx (lux).

2.2 Solar Spectrum

It is the surface temperature of the sun that mainly characterizes the solar spectrum. This spectrum defines the corresponding spectral irradiance for all wavelengths of sunlight. Visible light, with wavelengths between 0.4 µm and 0.75 µm, has a 46% share of the spectrum, infrared light 47%, and ultraviolet light only 7% (see Figure 1). The earth's atmosphere reduces the irradiance that reaches the earth's surface. Ozone, water vapor and carbon dioxide absorb radiation with certain wavelengths as it passes through the atmosphere. The significant reduction in mainly the ultraviolet and infrared parts of the spectrum is a result of this absorption.[15]

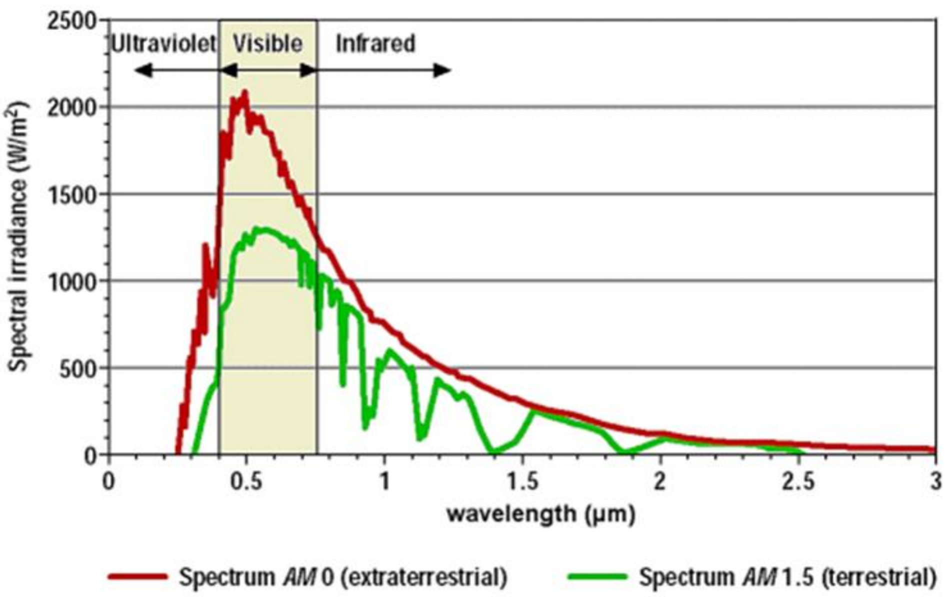

Figure 2.1: Trends of Spectral Irradiance to the wavelength of sunlight.

2.3 The Photovoltaic (PV) Effect And PV Cells

Without going too deep into semiconductor physics, the operation of the PV cells can be explained by using the energy band structure according to which the most weakly bonded electrons have energies in the energy band called the valence band. The next band with higher values of energy is called the conduction band. The energy separating the valence and conduction bands is called the band gap energy (Eg). When a sufficient amount of energy (> Eg) is applied to an electron in the valence band, the atomic bonds of the electron are broken and the electron is excited into conduction band and it is then free to conduct current through the material. When electron in excited into conduction band, an empty vacancy opens to the valence band where the electron used to be located creating a positive charge, a hole.

In case of a pure semiconductor material, after certain time the free electron will recombination, the free electron becomes trapped again in the atomic bonds of the material. This is why typical PV cells are composed of two different types of semiconductors, p- and n-type semiconductors. Different types of materials are created by introducing a small amount of impurity atoms (such as boron and phosphorus in case of silicon PV cells). When the two different materials are joined together, an electric field is created in the junction between the materials.

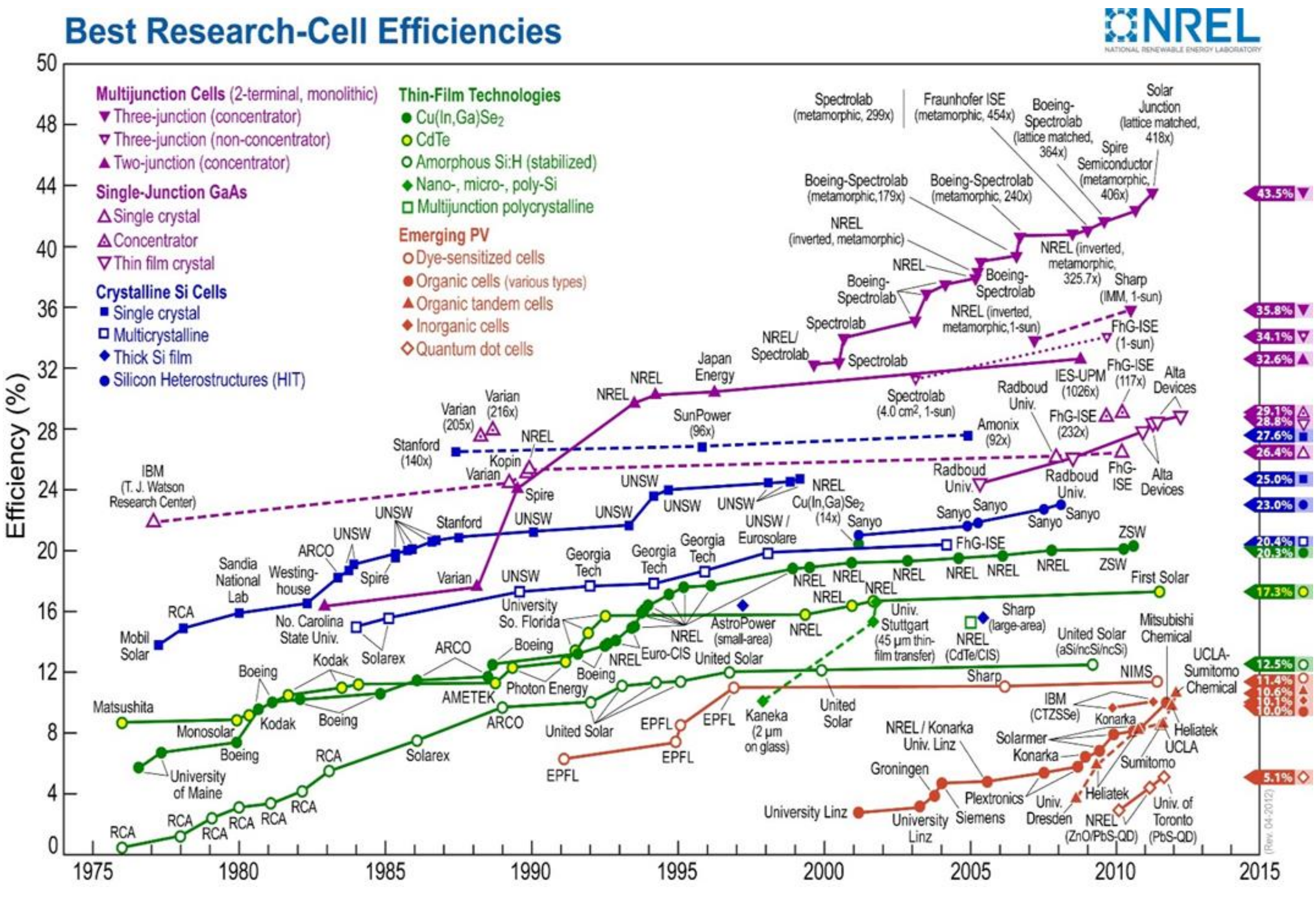

Figure 2.2: Development of the cell efficiencies over last 40 year. [16]

Photovoltaics is the direct conversion of light into electricity at the atomic level. Some materials exhibit a property known as the photoelectric effect that causes them to absorb photons of light and release electrons. When these free electrons are captured, an electric current results that can be used as electricity.

The photoelectric effect was first noted by a French physicist, Edmund Becquerel, in 1839, who found that certain materials would produce small amounts of electric current when exposed to light. In 1905, Albert Einstein described the nature of light and the photoelectric effect on which photovoltaic technology is based, for which he later won a Nobel Prize in physics. The first photovoltaic module was built by Bell Laboratories in 1954. It was billed as a solar battery and was mostly just a curiosity as it was too expensive to gain widespread use. In the 1960s, the space industry began to make the first serious use of the technology to provide power aboard spacecraft. Through the space programs, the technology advanced, its reliability was established, and the cost began to decline. During the energy crisis in the 1970s, photovoltaic technology gained recognition as a source of power for non-space applications.

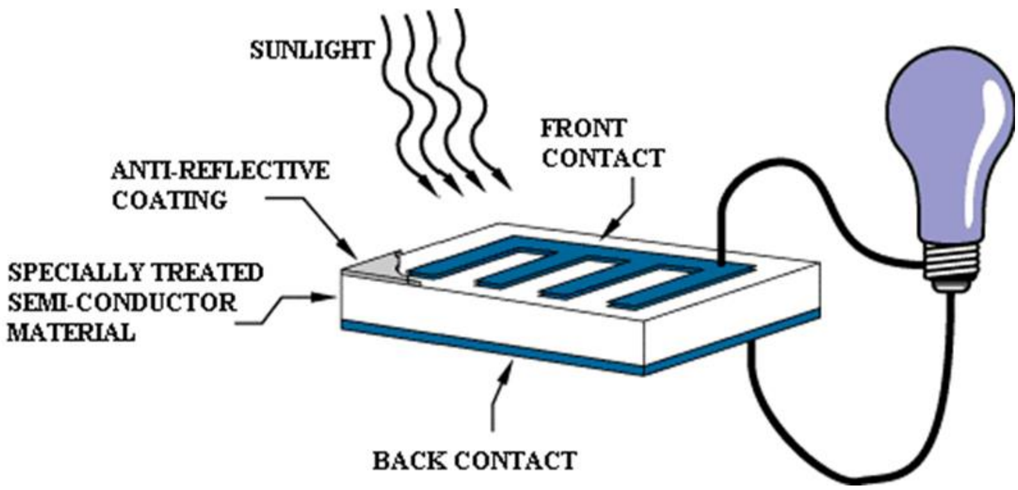

Figure 2.3: Simple solar cell

The diagram above illustrates the operation of a basic photovoltaic cell, also called a solar cell. [17] Solar cells are made of the same kinds of semiconductor materials, such as silicon, used in the microelectronics industry. For solar cells, a thin semiconductor wafer is specially treated to form an electric field, positive on one side and negative on the other. When light energy strikes the solar cell, electrons are knocked loose from the atoms in the semiconductor material. If electrical conductors are attached to the positive and negative sides, forming an electrical circuit, the electrons can be captured in the form of an electric current -- that is, electricity. This electricity can then be used to power a load, such as a light or a tool.

A number of solar cells electrically connected to each other and mounted in a support structure or frame is called a photovoltaic module. Modules are designed to supply electricity at a certain voltage, such as a common 12 volts system. The current produced is directly dependent on how much light strikes the module.

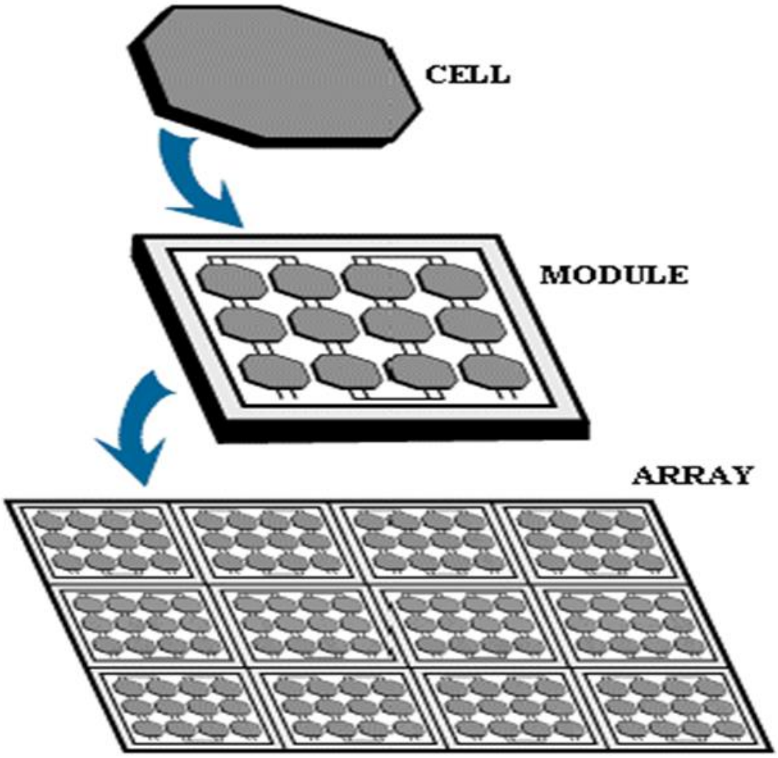

Figure 2.4: Development of array from cell.

Multiple modules can be wired together to form an array. In general, the larger the area of a module or array, the more electricity that will be produced. Photovoltaic modules and arrays produce direct-current (dc) electricity. They can be connected in both series and parallel electrical arrangements to produce any required voltage and current combination. Caption Today's can be seen for the most common PV devices use a single junction, or interface, to create an electric field within a semiconductor such as a PV cell. In a single-junction PV cell, only photons whose energy is equal to or greater than the band gap of the cell material can free an electron for an electric circuit. In other words, the photovoltaic response of single-junction cells is limited to the portion of the sun's spectrum whose energy is above the band gap of the absorbing material, and lower-energy photons are not used.

The efficiencies of currently the best research cells according to U.S. National Renewable Energy Laboratory (NREL, 2013) are shown in Fig 2.2.1. It can be seen that the highest reported efficiencies of 37.8% and 44% had been obtained in 2013 with three-junction PV cells under non-concentrated (InGaP/GaAs/InGaAs) and concentrated (GaInP/GaAs/GaInNAs) irradiances, respectively. According to Green et al. (2013), the best confirmed (under standard test conditions (STC) with an irradiance of 1000 W/m2 with AM1.5 spectrum and at a cell temperature of 25°C efficiency of a terrestrial PV module was 24.1% and it was obtained with a thin film PV module based on GaAs.[17]

2.4 How Shade Affects a Solar Array

When assessing the speed and proliferation with which solar power has become a mainstream technology, it's interesting to note how poorly understood certain aspects of the technology still are. When harvesting sunlight, shade and shadows being cast upon the collection surface is a major problem, however if one were to ask their local solar installer about how shade will affect their solar output, most wouldn't be able to provide a meaningful answer beyond, "it's not good."

This lack of understanding isn't just limited to the installers, as solar and electrical engineers answer nearly the same when put on the spot. Just about everyone finds this vague response to be concerning, so we sought out a better answer. Over the course of a 6-month study on shading in 2011, we were able to quantify and ultimately simulate the effects of shading on a solar array.

As it turns out, the effects can differ significantly from both the specific equipment used and the overall design and orientation of the array, so we did what we could to approach the problem from a generic standpoint about shading itself and focus less on design-specific effects.

It starts off simple enough…

There are two distinct forms of shading that we've come to describe as "soft" and "hard" shading.

Soft shading can be described as simply lowering the intensity of the irradiance levels, without causing any form of visible separation of shaded and unshaded regions. A great example of soft shading would be due to cirrus or stratus clouds evenly blocking out some, but not all of the sunlight. Soft shading cast on a PV cell will cause the cell's current output to proportionally drop. As long as there is enough light (~50W/m2), the voltage output of the cell will remain unchanged and only the current output will diminish. The voltage of the PV cell depends more on temperature and the electron band-gap in the materials than on the light itself.

Hard shading is created when a physical object, such as a telephone pole, or tree is physically obstructing the sunlight, creating obvious visible regions of lit and unlit cells on the array. It's a lot more difficult to describe how hard shade affects a PV cell, as the physical geometry of the shade comes into play. As long as there is a solid strip or channel of illuminated material between two electrodes on a PV cell, there will be some electric current. The current is proportional to the surface area of the cell that was illuminated and the shape of the shadow does not appear to matter as much as the area of the shadow.

However, certain shapes of shading would create narrow areas of illumination in which the current would squeeze and be focused in the narrow illuminated portions of the cell, creating areas of extremely high temperature, known in the industry as "hot spots." These hot spots in very rare cases have been known to cause burn-outs and small fires within modules, as they may have the current from an entire module being pinched into a very tiny area of solar cell.

If there is no complete illuminated path between electrodes or the entire cell is shaded, then no current will flow through the cell, and its voltage output will collapse. This has the effect of "opening" the circuit, as there is no longer a complete path for the electrons to travel.

Most modern solar cells are designed to lower the odds of this effect by imprinting silver leads across the cell. This is an attempt to provide more possible paths for an electron to take across the silicon, much the same way that a freeway allows more rapid travel through a densely packed city. As a result, as long as these silvered-cells have any light exposed to them, they will generate power.

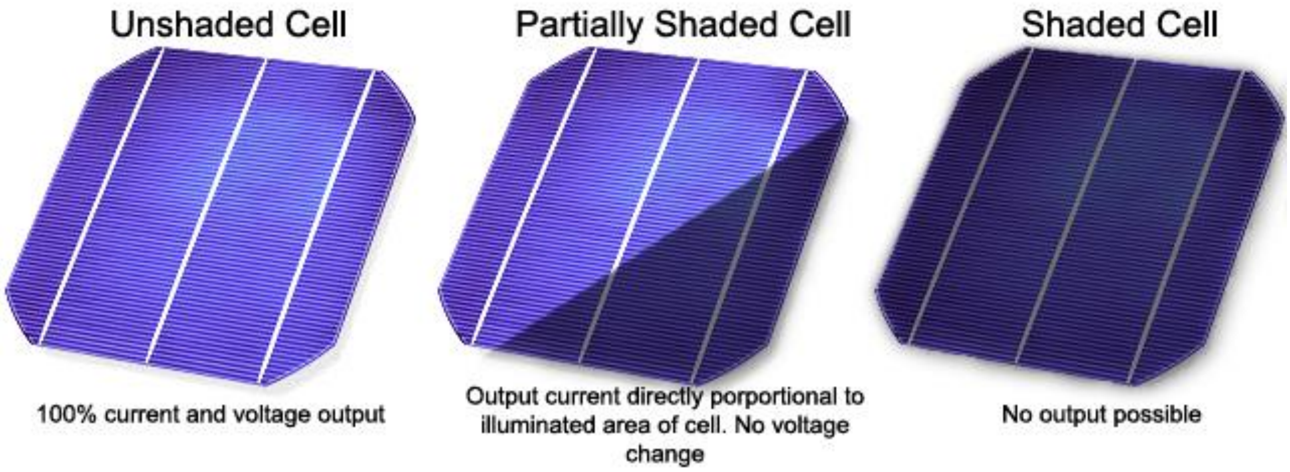

Figure 2.5: Solar cells in different shading condition. [18]

Some module manufacturers, such as Sun power, find alternative solutions to using the silvered leads, and create their solar cells using a different process.

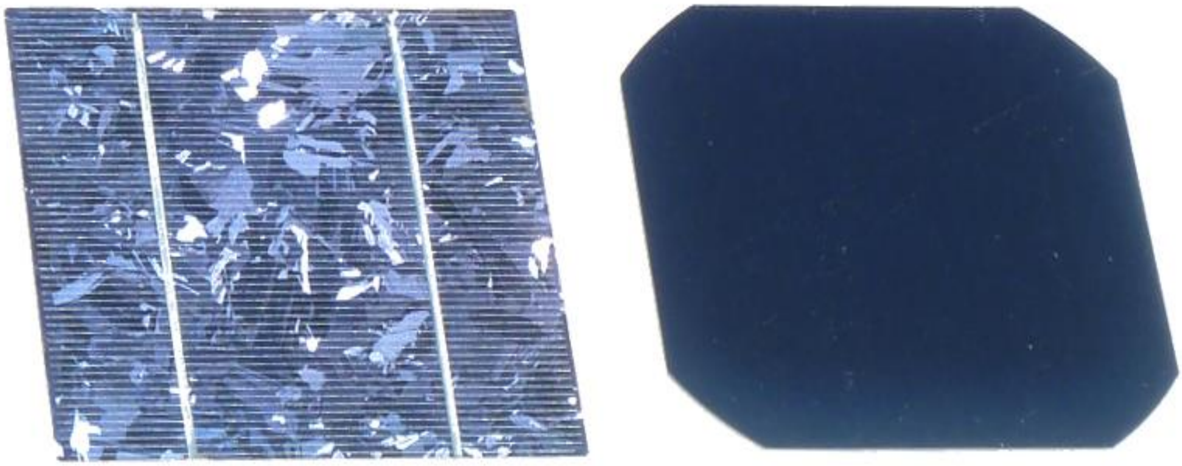

Figure 2.6: Silver lead solar cells.

The apparent tradeoff is that they sacrifice reliability in the field environment in preference for higher performance under ideal conditions.

At the module level, several solar cells are connected in series, in order to increase their output voltage. Soft shade, cast on a module will still allow voltage to be generated, but less current will flow from the module. Hard shade cast on a portion of the area on a solar module will open the circuit, causing the voltage generated by the module to drop.

Modern solar modules come with small components inside them called “bypass diodes.” These diodes allow shaded cells to be bypassed, allowing the current from other modules in the string to continue flowing. There are downsides, however, as not every cell can have its own bypass diode, which usually results in a third to a half of the module being bypassed if even one cell is completely shaded.

Strings of modules are again connected in series, where the current must be the same throughout all components. That means that without the bypass diodes, any shade on any cell in the string would cause the entire string to stop producing power entirely. Such a devastating loss of power had to be avoided, so typically three diodes are placed in along the solar cells. The diodes are placed in such a way they will allow current to flow through them only if the solar cells they bypass are shaded and opened. Since the diodes have a negligible voltage drop, there are very little losses induced by the diodes, so the only real loss from a shaded group of cells is whatever voltage they were providing.

A great way to visualize the way in which different types of shade effect the module is by looking at the effect on the modules I-V curve, or mathematical curve representing the module’s possible current and voltage output.

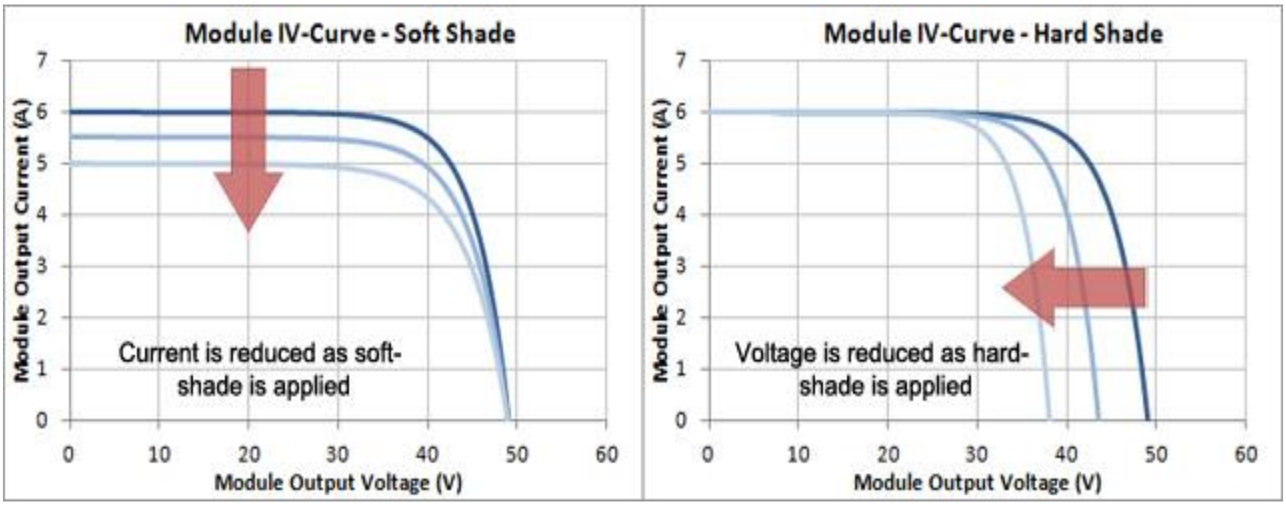

Figure 2.7: Shaded IV curves in Soft-Shade and Hard-Shade.

The IV curve is a common tool by which solar engineers can convey information regarding the input or output operation ranges of a device. It is a graph of the output current delivered from the module as a function of the output voltage applied to the module (based on the resistive load applied). The curve’s shape is important, because when multiplied again by the voltage, the IV curve becomes a PV (power and voltage) curve, displaying the output power as a function of the voltage of the module.

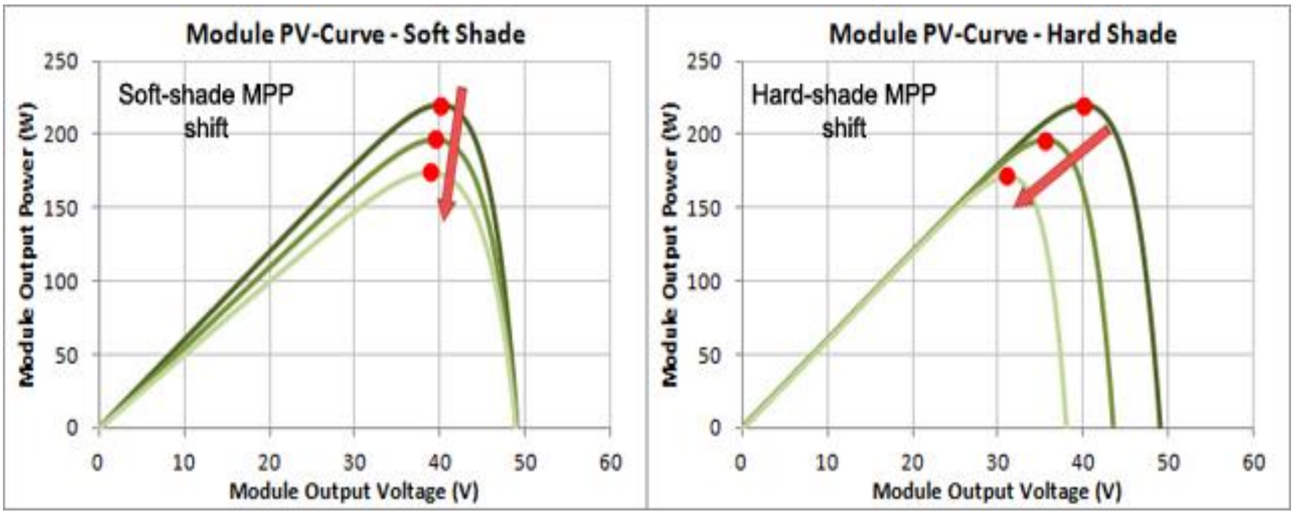

Figure 2.8: Shaded Power-Voltage curve in Soft-Shade and Hard-Shade.

For every module, there is a point on its PV curve that is higher than any other point, at a specific voltage. This is called the “maximum power point” and it is important because the solar inverter is designed to seek out this point as best it can, in order to most effectively deliver the most power to the grid. However, as the graphs above show, the effects of shade cause this point to shift around.

As a result, whenever shade is applied to a solar array, the inverter loses the ability to deliver the optimal amount of power, and must begin shifting its power-tracking point around, trying to find the new “max power point.” All of this behavior on the part of the inverter has the nasty effect of drastically reducing the array’s output power for a few minutes.

Up until now, we’ve only been discussing the effects of a single module. So how can these two types of shade interact with the performance of an entire array? Since the shadows are almost never evenly spread over every module in the array, mismatching outputs between modules in a string and strings in the array are induced. From the two different types of shade applied, again two different effects occur.

Soft shade applied on some modules in a string and not evenly to others will cause an effect called “current mismatch,” where the current output of each module is varied. Since the laws of electricity dictate that all components connected in series must have the same current, what typically results is the string settles on the output of the lowest-performing module, reducing the output of the entire string to that of the most heavily-shaded cell in the string. This same effect occurs independently for all strings in an array, as strings are connected in parallel. However, despite being independent to each string, current imbalance in one string can still negatively affect other strings, through interaction with the inverter.

Hard shade, on the other hand, causes the output voltage of the shaded modules to drop, however thanks to the bypass diodes and the inverter, the current output typically remains the same unless all modules are affected. However, when two or more strings connected in parallel have shade unevenly applied to them, an effect called “voltage mismatch” occurs. Voltage mismatch is the condition in which two parallel strings are outputting different voltages when measured independently. This can have a confusing effect on the inverter, which sees a much more complicated and messy curve as it adjusts its load, ever seeking the most optimal output.

It is important to note that voltage mismatch cannot occur on a single-string solar array, as there are no parallel string connections with which to create an "imbalance." A solar array consisting of only one string of modules can only have current-mismatch effects applied to it. Casting hard shade on a single string will drop the voltage of the string, but the inverter will detect this drop and quickly adjust, seeking the new maximum power point.

As for the effects of these two different mismatches on the inverter, several outcomes are possible, depending on the software behavior of the inverter. The PV curve of the entire array exists as the series sum of the modules and the parallel sum of the strings. A shadow moving over the surface of several modules over time has the effect of constantly changing the PV curve from one smooth peak to more of a mountain range.

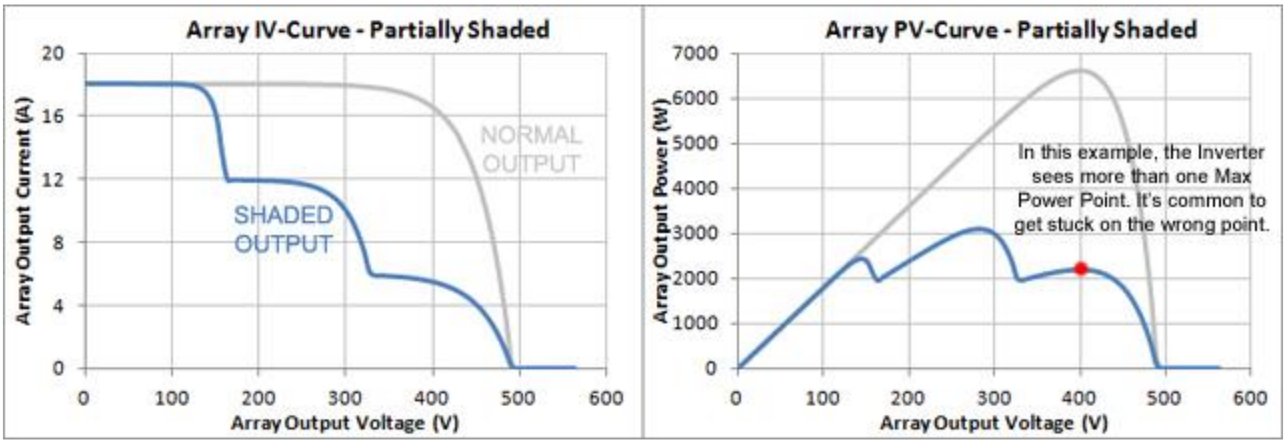

Figure 2.9: Inverter mpp curves in partially shading condition.

As the peaks of the PV curve in the inverter change from the shade, the electronics that track the maximum power point can become confused or lost, causing the inverter to choose to operate for long periods of time well outside the optimal output range. This can cause significant loss of power output and eventually annual energy yield. There have been notable advancements in the methods and electronics of the inverters, as well as the birth of new technologies in order to deal with the complications brought on by shade. A great example of this development is the inclusion of two or more MPPT channels in popular residential inverters.

Micro-inverters are inverters that are installed on a single module, allowing each module to independently generate AC electricity at its own optimal rate regardless of whether its neighbors are shaded or not. While these alternatives have recently appeared in the solar market, the downsides to this approach are the sizable expense and the relative inefficiency of these micro-inverters. As this technology develops it appears to already be converging on the emergence of "AC-modules," or solar modules that have integrated inverters and output alternating current directly onto the grid.

Power-optimizers have also been created as a niche answer to the problems caused by shade, but their relative complexity and need to be extremely efficient price them out of the range of practicality. They work similarly to the micro-inverters, isolating each module's performance from the hindrance of the others, but don't go so far as to convert the electricity into grid-compatible power.

To put it simply: anything an optimizer can do, a micro-inverter can do as well, but the micro-inverter gets away with less overall hardware.

In terms of providing a simple answer to the shade question, the unfortunate finding to our research was that we would need the assistance of a computer in order to fully mathematically model what was going on at the PV-cellular level in order to get an accurate picture of array behavior as a whole. Since the time of this study, we have developed several such software packages and tools to assist with achieving reliable performance results; however it seems that the industry as a whole has maneuvered around the question by relying entirely on the results of PV-WATTS, a software tool developed by National Renewable Energy Laboratories (NREL).

A solar PV system consists of one or several solar PV modules, each consisting of multiple PV cells. The PV cells generate electrical energy directly from sunlight by taking advantage of the PV effect (Lorenzo et al. 1994). The most commonly used PV cell is constructed from p-type and n-type silicon (Figure 3). When these two types of silicon are placed in close contact with each other this creates a semiconductor material. When the semiconductor material is exposed to sunlight, electrons are knocked loose from the n-type silicon. If the two sides are connected, forming an electrical circuit, the moving electrons can be used as electric current (Lorenzo et al. 1994).

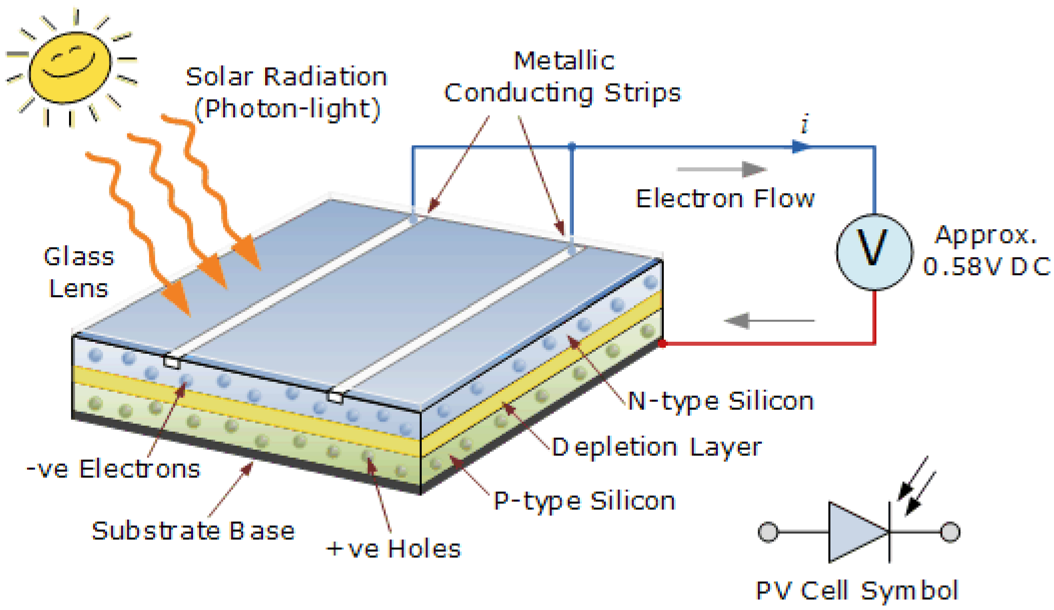

Figure 2.10: An illustration of photovoltaic electricity generation

Under normal conditions, when each cell in a solar module receive the same amount of sunlight they generate roughly the same amount electricity (there is always some difference in output due to variation in cell quality, as is expected from the manufacturing process). Under conditions with uneven shading, a shaded cell will allow current from other unshaded cells to pass through its parallel resistance, resulting in a reverse voltage and potentially a major drop in power output (Chakraborty, 2013). The unshaded cells are still generating power, but the shaded cell (s) will now absorb power instead (Figure 4). The shaded cell will receive a (high) current from the accumulated generation of all unshaded cells, leading to a high reversed terminal voltage, and thus a high absorbing power, on the shaded cell. This can lead to damage to the shaded PV cell, causing permanent generation loss to the system. (Chakraborty, 2013; Zheng et al., 2013).

2.5 Mathematical Presentation For The Operation Of Photovoltaic Cells

Mathematical presentation for the I-V characteristic of a PV cell can be derived based on extensive knowledge of semiconductor physics (Luque and Hegedus, 2003). The general expression for the current of a PV cell I is

$$I = I_{SC} - I_{01}[exp^{(\frac{qV}{kT})} - 1] - I_{02}[exp^{(\frac{qV}{2kT})} - 1] \text{ -------------------------------- } (2.4.1)$$

Where I_{SC} is the Short Circuit Current, V is the Voltage, k is the Boltzmann Constant, q is the elementary charge, T is the temperature, I_{01} and I_{02} the dark saturation currents in the quasi-neutral and depletion regions of the cell, respectively. Equation (2.4.1) neglects the effects of parasitic series resistance R_s and the shunt resistance R_{sh}. These resistances are typically associated with real PV cells and they represent losses due to several reasons. [19] Incorporating the resistances into Eq. (2.4.1) yields,

$$I = I_{ph} - I_{01}[exp^{(\frac{V+IR_S}{V_t})} - 1] - I_{02}[exp^{(\frac{V+IR_S}{2V_t})} - 1] - \frac{V+IR_S}{R_{sh}} \text{ ------------- } (2.4.2)$$

Where, V_t = kT/q, is the thermal voltage of the cell. An electrical equivalent circuit diagram shown in Figure. 2.12 can be drawn based on Eq. (2.4.1). This model is widely used in the literature. [20]; [21]; [22] .

.

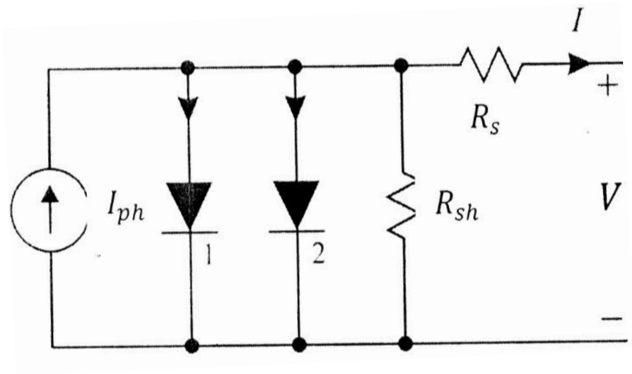

Figure 2.11: The electrical equivalent circuit diagram of a PV cell based on the two-diode model.

Often it is assumed that the dark saturation current in the depletion layer is relevantly small (shown in Figure-2.11). It is a reasonable assumption in case of high quality PV cells. [23] The effects of both diodes are then taken into account by using ideality factor A. Combining the effets of the diodes by using ideality factor, A yields the well-known one-diode model in which the current of the PV cell.

$$I = I_{ph} - I_0 \left[exp^{\left(\frac{V+IR_S}{AV_t}\right)} - 1 \right] - \frac{V+IR_S}{R_{sh}} \text{---(2.4.3)}$$

Where, I_0 is the dark saturation current.

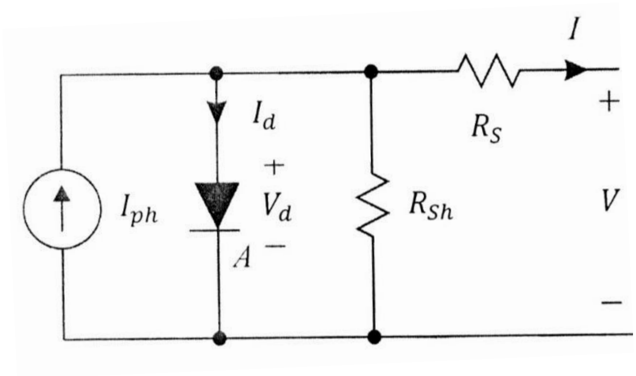

Figure 2.12: The electrical equivalent circuit diagram of a PV cell based on the one-diode model.

One diode model is widely used in the literature, because it is easier to use than the two-diode model to mathematically model the operation of PV cells and modules. In Figure – 2.12, I_d are the current and V_d = V+IR_S the voltage of the diode. I_d is the product of the dark saturation current I_0 and the exponential term subtracted by one in Equation 2.4.3.

The equivalent circuit diagram in Figure 2.12 consists of a current source representing the light generated current which is directly proportional to the amount of irradiance reaching the surface of a PV cell is also dependent on the operating temperature of the cell. This simplified model is well-known and widely used in the literature.

2.6 Some Definitions Related To Solar Radiation

The sun's structure and characteristics determine the nature of the energy it radiates into space. The first major topic in this chapter concerns the characteristics of this energy outside the earth's atmosphere, its intensity, and its spectral distribution.

Solar geometry is also discussed here, that is, the position of the sun in the sky, the direction in which beam radiation is incident on surfaces of various orientations, and shading. The third topic is extraterrestrial radiation on a horizontal surface, which represents the theoretical upper limit of solar radiation available at the earth's surface.

2.6.1 The Solar Constant

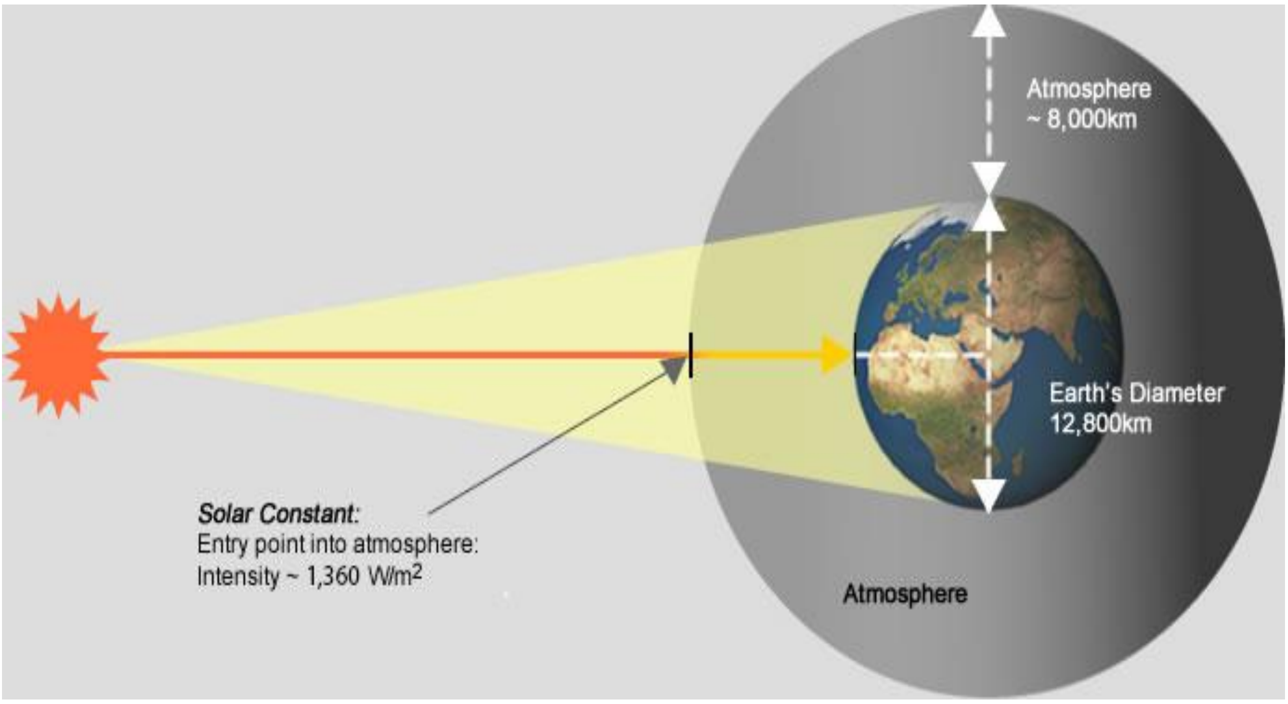

Figure 2.13: The Solar Constant (Adopted from Green Rhino Energy)

The solar constant, a measure of flux density, is the conventional name for the mean solar electromagnetic radiation (the solar irradiance) per unit area that would be incident on a plane perpendicular to the rays, at a distance of one astronomical unit (AU) from the Sun (roughly the mean distance from the Sun to the Earth). The solar constant includes all types of solar radiation, not just the visible light. It is measured by satellite as being 1.361 kilowatts per square meter (kW/m^2) at solar minimum and approximately 0.1% greater (roughly 1.362 kW/m^2) at solar maximum.[1] The solar "constant" is not a physical constant in the modern CODATA scientific sense; it varies in value, and has been called a "misconception". It has been shown to vary historically in the past 400 years over a range of less than 0.2 percent.

2.6.2 Extraterrestrial Radiation

Extraterrestrial radiation (w/m^2) is the intensity (power) of the sun at the top of the Earth's atmosphere. It is usually expressed in irradiance units (Watts per square meter) on a plane normal to the sun.

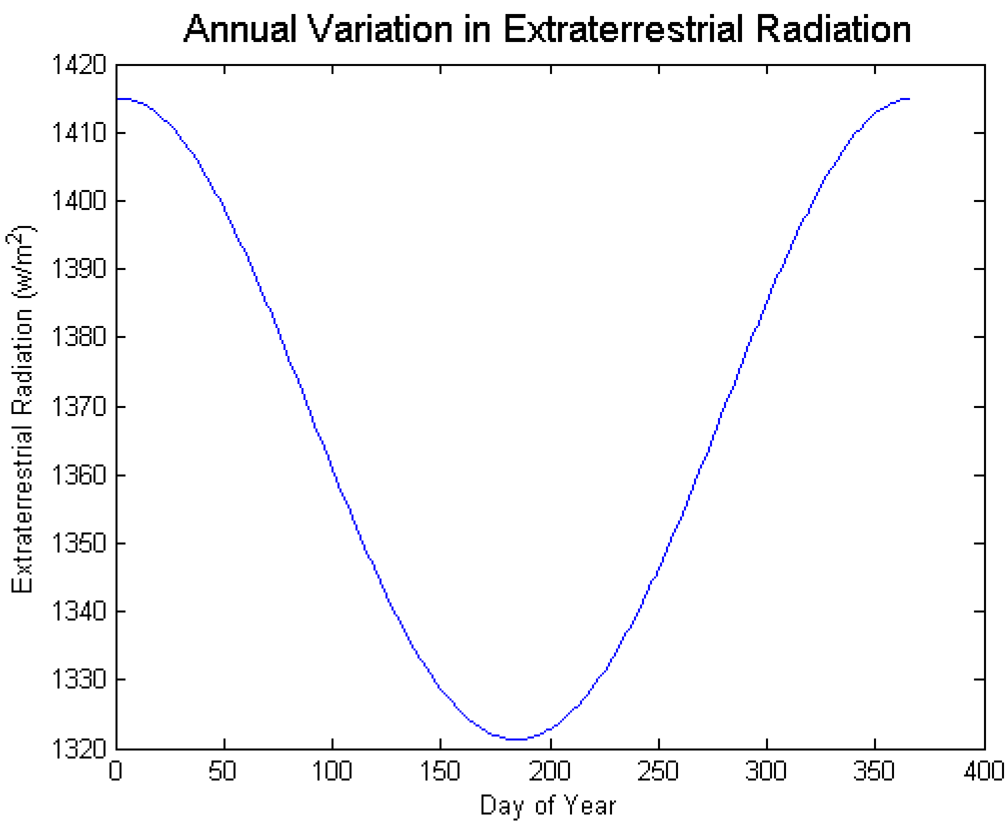

Figure 2.14: Variation of extraterrestrial solar radiation with the days of year

(Adopted from PVPerformance Modelling Collaborative)

2.6.3 Air Mass m

The air mass coefficient defines the direct optical path length through the Earth's atmosphere, expressed as a ratio relative to the path length vertically upwards, i.e. at the zenith. The air mass coefficient can be used to help characterize the solar spectrum after solar radiation has traveled through the atmosphere. The air mass coefficient is commonly used to characterize the performance of solar cells under standardized conditions, and is often referred to using the syntax "AM" followed by a number. "AM1.5" is almost universal when characterizing terrestrial power-generating panels.

2.6.4 Diffuse Radiation

Diffuse sky radiation is solar radiation reaching the Earth's surface after having been scattered from the direct solar beam by molecules or suspensions in the atmosphere. It is also called skylight, diffuse skylight, or sky radiation and is the reason for changes in the color of the sky. Of the total light removed from the direct solar beam by scattering in the atmosphere (approximately 25% of the incident radiation when the sun is high in the sky, depending on the amount of dust and haze in the atmosphere), about two-thirds ultimately reaches the earth as diffuse sky radiation.[citation needed] When the sun is at the zenith in a cloudless sky, with 1367 W/m2 above the atmosphere, direct sunlight is about 1050 W/m2, and total insolation about 1120 W/m^2. This implies that under these conditions the diffuse radiation is only about 70 W/m^2 out of the original 1367 W/m^2.

2.6.5 Total Solar Radiation

Total solar irradiance is defined as the amount of radiant energy emitted by the Sun over all wavelengths that fall each second on 11 sq ft (1 sq m) outside the earth's atmosphere. By way of further definition, irradiance is defined as the amount of electromagnetic energy incident on a surface per unit time per unit area. Solar refers to electromagnetic radiation in the spectral range of approximately 1-9 ft (0.30-3 m), where the shortest wavelengths are in the ultraviolet region of the spectrum, the intermediate wavelengths in the visible region, and the longer wavelengths are in the near infrared. Total means that the solar flux has been integrated over all wavelengths to include the contributions from ultraviolet, visible, and infrared radiation.

2.6.6 Irradiance

In radiometry, irradiance is the radiant flux (power) received by a surface per unit area. The SI unit of irradiance is the watt per square meter (W/m^2). The CGS unit erg per square centimeter per second ($erg \cdot cm^{-2} \cdot s^{-1}$) is often used in astronomy. Irradiance is often called "intensity" in branches of physics other than radiometry, but in radiometry this usage leads to confusion with radiant intensity. Spectral irradiance is the irradiance of a surface per unit frequency or wavelength, depending on whether the spectrum is taken as a function of frequency or of wavelength. The two forms have different dimensions: spectral irradiance of a frequency spectrum is measured in watts per square meter per hertz ($W \cdot m^{-2} \cdot Hz^{-1}$), while spectral irradiance of a wavelength spectrum is measured in watts per square meter per meter ($W \cdot m^{-3}$), or more commonly watts per square meter per nanometer ($W \cdot m^{-2} \cdot nm^{-1}$).

2.6.7 Irradiation

Irradiation is the process by which an object is exposed to radiation. The exposure can originate from various sources, including natural sources. Most frequently the term refers to ionizing radiation, and to a level of radiation that will serve a specific purpose, rather than radiation exposure to normal levels of background radiation. The term irradiation usually excludes the exposure to non-ionizing radiation, such as infrared, visible light, microwaves from cellular phones or electromagnetic waves emitted by radio and TV receivers and power supplies.

2.6.8 Insolation

Insolation is the solar radiation that reaches the earth's surface. It is measured by the amount of solar energy received per square centimeter per minute. Insolation affects temperature. The more the insolation, the higher the temperature. In any given day, the strongest insolation is received at noon. Factors affect insolation (without the effect of the atmosphere):

1. Angle of the sun
2. Distance between the sun and the earth
3. Duration of daylight

The longer the duration of daylight, the more the insolation received per day.

2.6.9 Radiosity Or Radiant Existence

Radiosity is a method of rendering based on an detailed analysis of light reflections off diffuse surfaces. The images that result from a radiosity renderer are characterized by soft gradual shadows.

2.6.10 Emissive Power Or Radiant Self-Existence

The energy of thermal radiation emitted in all directions per unit time from each unit area of a surface at any given temperature.

2.6.11 Solar Time

Time based on the rotation of the Earth with respect to the Sun. Solar time units are slightly longer than sidereal units due to the continuous movement of the Earth along its orbital path. For example, by the time the Earth has completed one full rotation on its axis with respect to the fixed stars, it has also moved a short distance in its orbit and is oriented slightly differently to the Sun, so that it must turn slightly more on its axis to complete a full rotation with respect to the Sun. The time it takes the Earth to rotate fully with respect to the Sun is called a solar day.

The length of a solar day varies throughout the year due to variations in the Earth's orbital speed and other factors. The average value of all solar days in the solar year is called a mean solar day; it is 24 hours long and by convention is measured from midnight to midnight. A solar year is the period of time required for the Earth to make a complete orbit with respect to the Sun as measured from one vernal equinox to the next; it is equal to 365 days, 5 hours, 48 minutes, 45.51 seconds. A solar year is also called an astronomical year and a tropical year. A solar month is one twelfth of a solar year, totaling 30 days, 10 hours, 29 minutes, 3.8 seconds.

2.6.12 Direction Of Beam Radiation

The geometric relationships between a plane of any particular orientation relative to the earth at any time (whether that plane is fixed or moving relative to the earth) and the incoming beam solar radiation, that is, the position of the sun relative to that plane, can be described in terms of several angles (Benford and Bock, 1939). Some of the angles are indicated in figure – 2.7. The angles and a set of consistent sign conventions are as follows:

2.6.13 Latitude, Ø

The angular distance of a place north or south of the earth's equator, or of a celestial object north or south of the celestial equator, usually expressed in degrees and minutes.

2.6.14 Declination, δ

In astronomy, declination (abbreviated dec; symbol δ) is one of the two angles that locate a point on the celestial sphere in the equatorial coordinate system, the other being hour angle. Declination's angle is measured north or south of the celestial equator, along the hour circle passing through the point in question.

Declination in astronomy is comparable to geographic latitude, projected onto the celestial sphere, and hour angle is likewise comparable to longitude.[3] Points north of the celestial equator have positive declinations, while those south have negative declinations. Any units of angular measure can be used for declination, but it is customarily measured in the degrees (°), minutes ('), and seconds (") of sexagesimal measure, with 90° equivalent to 1⁄4 circle. Declinations with magnitudes greater than 90° do not occur, because the poles are the northernmost and southernmost points of the celestial sphere.

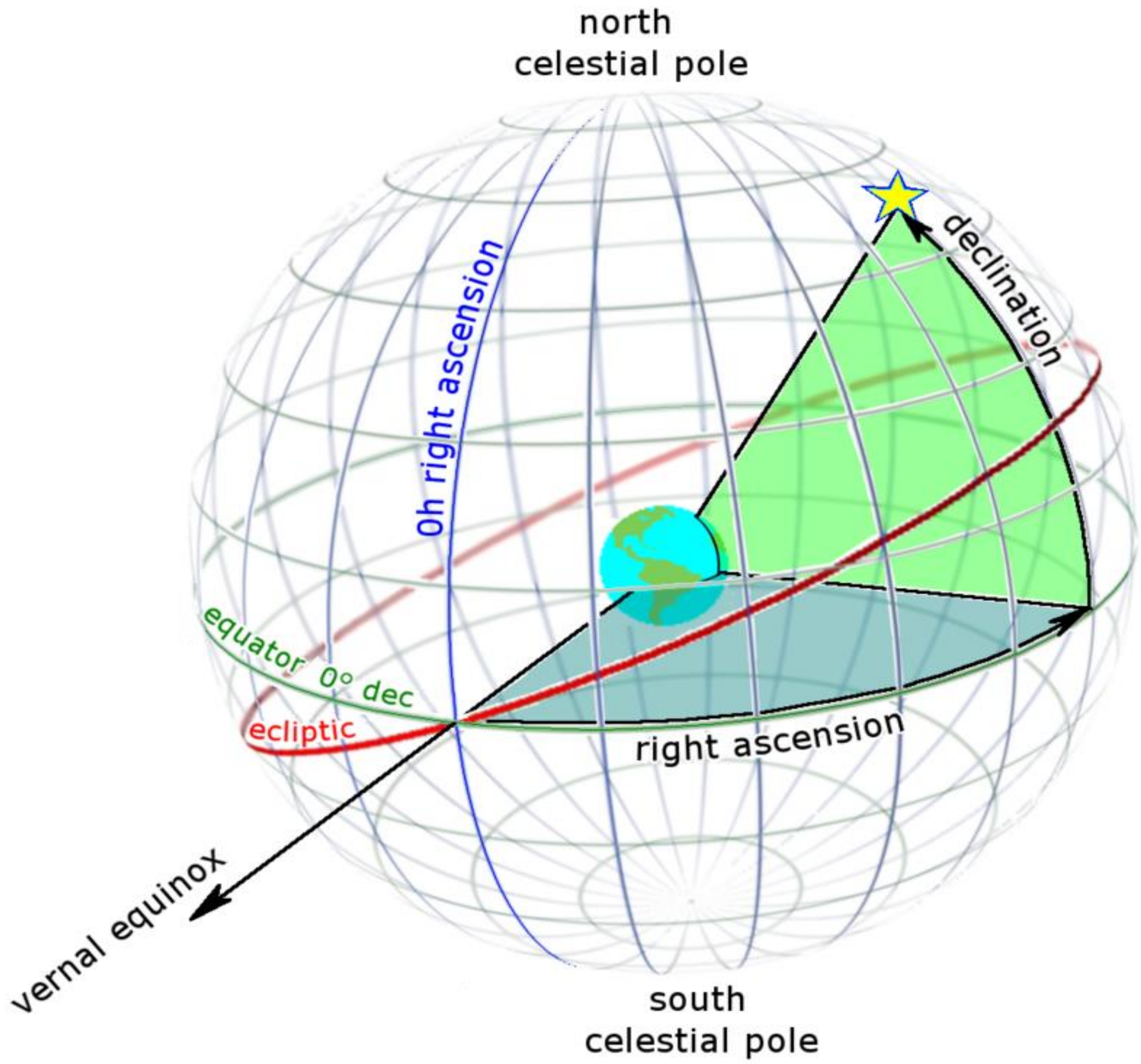

Figure 2.15: Sun Declination Angle, δ.

An object at the

a) Celestial equator has a declination of 0°

b) North celestial pole has a declination of +90°

c) South celestial pole has a declination of −90°

The sign is customarily included whether positive or negative.

2.6.15 Surface Azimuth Angle, β

An azimuth, meaning "the directions" is an angular measurement in a spherical coordinate system. The vector from an observer (origin) to a point of interest is projected perpendicularly onto a reference plane; the angle between the projected vector and a reference vector on the reference plane is called the azimuth.

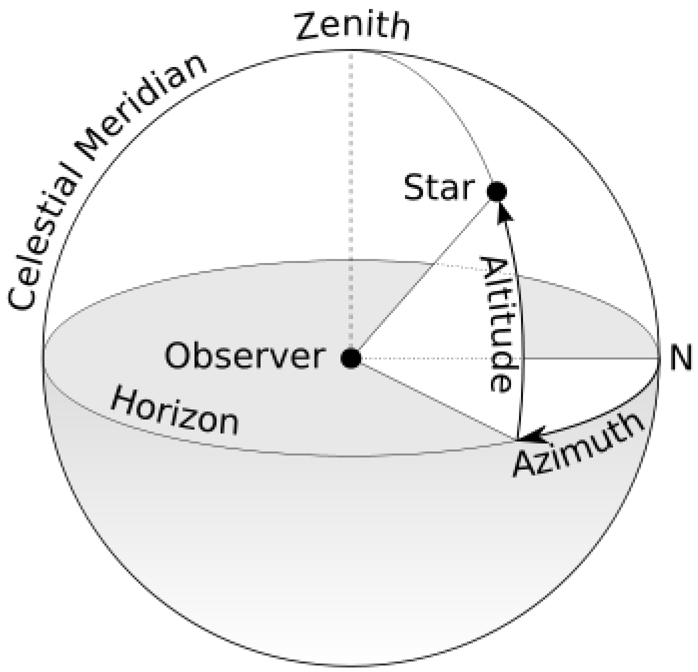

Figure 2.16: Surface azimuth angle.

2.6.16 Hour Angle, ω

In astronomy and celestial navigation, the hour angle is one of the coordinates used in the equatorial coordinate system to give the direction of a point on the celestial sphere. The hour angle of a point is the angle between two planes: one containing the Earth's axis and the zenith (the meridian plane), and the other containing the Earth's axis and the given point (the hour circle passing through the point).

As seen from above the Earth's north pole, a star's local hour angle (LHA) for an observer near New York (red). Also depicted are the star's right ascension and Greenwich hour angle (GHA), the local mean sidereal time (LMST) and Greenwich mean sidereal time (GMST). The symbol ϒ identifies the vernal equinox direction.

The angle may be expressed as negative east of the meridian plane and positive west of the meridian plane, or as positive westward from 0° to 360°. The angle may be measured in degrees or in time, with 24h = 360° exactly.

In astronomy, hour angle is defined as the angular distance on the celestial sphere measured westward along the celestial equator from the meridian to the hour circle passing through a point.[1] It may be given in degrees, time, or rotations depending on the application

2.6.17 Solar Noon

Solar noon is when the sun crosses the meridian and is at its highest elevation in the sky, at 12 o'clock apparent solar time. The local or clock time of solar noon depends on the longitude and date. The opposite of noon is midnight.

2.6.18 Zenith Angle θ_Z:

The solar zenith angle is the angle between the zenith and the center of the sun's disc. The solar elevation angle is the altitude of the sun, the angle between the horizon and the center of the sun's disc.

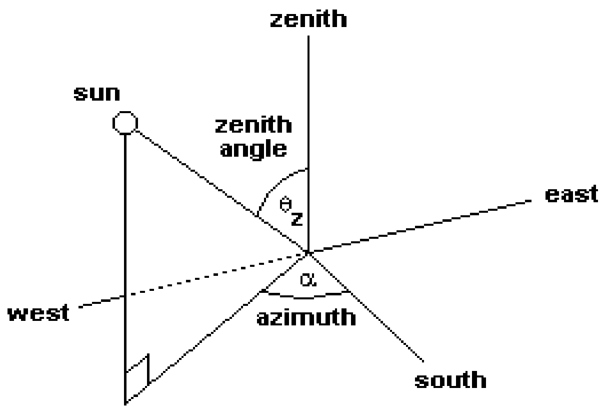

Figure 2.17: Zenith angle (Adopted from ATMOSPHERIC BOUNDARY LAYER SCIENCE)

2.6.19 Solar Altitude Angle, α_S

The solar elevation angle is the altitude of the sun, the angle between the horizon and the center of the sun's disc. Since these two angles are complementary, the cosine of either one of them equals the sine of the other. They can both be calculated with the same formula, using results from spherical trigonometry.

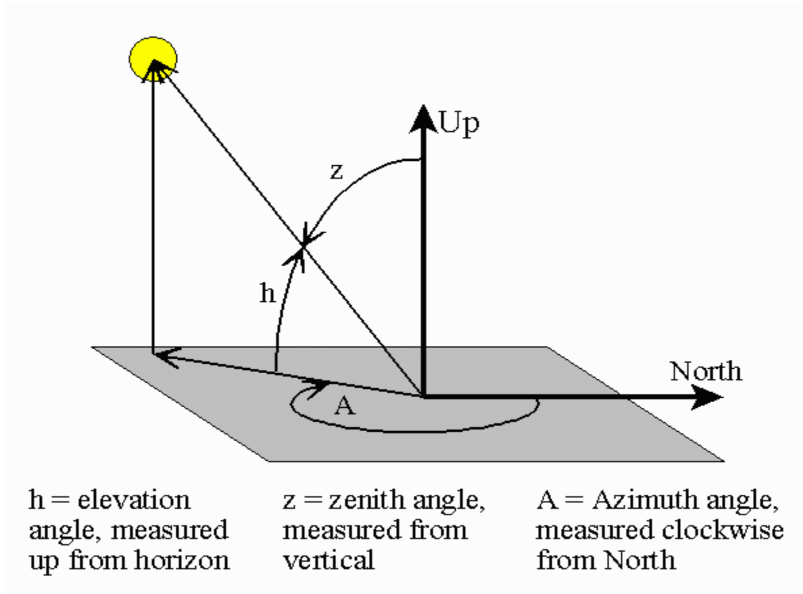

Figure 2.18: Solar altitude angle (Adopted from ESRL global monitoring division)

2.6.20 Solar Azimuth Angle, γ_S:

The solar azimuth angle is the azimuth angle of the sun. It defines in which direction the sun is, whereas the solar zenith angle or its complementary angle solar elevation defines how high the sun is.

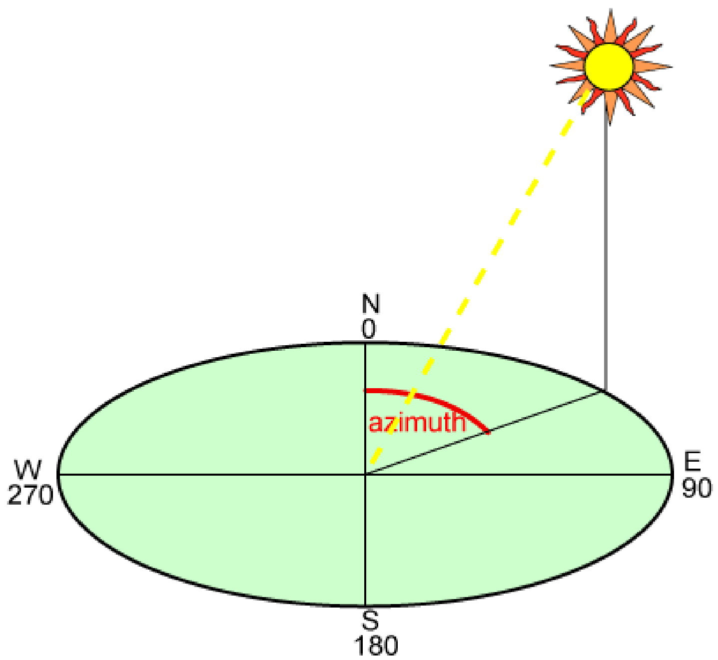

Figure 2.19: Solar Azimuth Angle, β (Adopted from PVEducation.ORG)

CHAPTER 3

METHODOLOGY FOR OBTAINING HOURLY SHADOW LENGTH

3. Methodology For Obtaining Hourly Shadow Length

The photovoltaic (PV) panels are arranged in many rows with some spacing mainly for installation purpose and later on for maintenance purposes. Shading on PV panels can significantly reduce system performance life time too. When an array of PV panels are connected in series, shading on even one module in the array can reduce the performance of the array as if all panels were shaded.

The earth revolves around the sun at a rate of one revolution every year and the earth also rotates cause a change in the incident angle of solar radiation on the PV panels. The clearance between two rows has kept during installation for maintenance and other issues varies from geographical region to region (for variation of latitude angle) and even varies in different day in a year (due to declination angle).

Variation of angle of incidence ϴ, causes a variation in the shadow length which has different values in different season. The shadow length of a tilted or vertically positioned solar panel can be said as the function of the position of sun during sunshine hours. This chapter will derive mathematical relationship between shadow length, solar azimuth angle, solar declination angle, solar altitude angle.

To derive a mathematical relationship the author adopts the mathematical approach from P. Biswas et al. 2009; which will help us to correlate out mathematical expressions.

Finding out the maximum shadow length, three consecutive steps can be covered.

3.1 Basic description

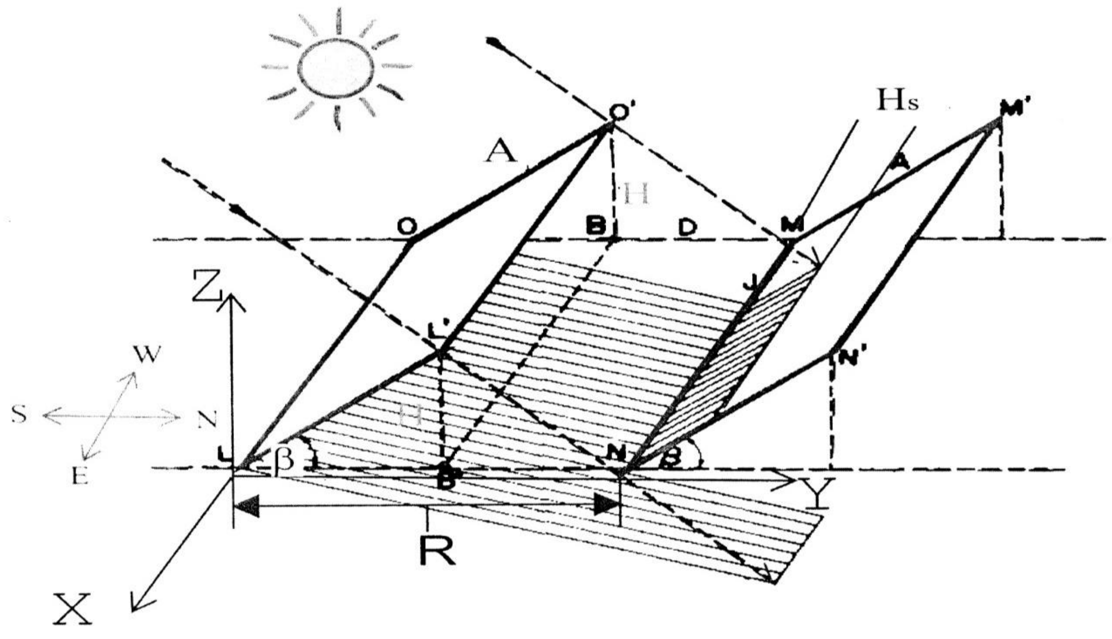

Figure 3.1: Position of two inclined solar PV modules with a tilt angle.

Non-tracking south inclined PV mounting setup is considered for this calculation. For this analysis capital of Bangladesh is considered. For the Dhaka city, calculation of hourly shadow length of the PV module setup requires determination of hourly sun's trajectory throughout a year. With the help of hourly value of azimuth angle and solar altitude, the sun's position can be tracked. Once the angles are known, using trigonometry the hourly value of shadow distance has been calculated throughout the year for a particular city.

In this way, the hourly shadow distances have been noted and maximum shadow length has been found out which gives the idea of minimum spacing between the solar PV module setup in Dhaka. By changing the design criteria sunshine hours changes in required spacing between the rows can be found.

3.2 Calculation of angles:

Solar altitude: Solar altitude is the angle between the horizontal plane and the Sun's rays.

$$\alpha = \sin^{-1}[\sin(\varnothing)\sin(\delta) + \cos(\varnothing)\cos(\delta)\cos(\omega)] \quad (3.2.1)$$

Where, Ø is the latitude of the region (°)

δ is the solar declination angle (°)

ω is the hour angle of the place (°)

The declination is the angular position of the sun at solar noon with respect to the plane of the equator

$$\delta = 23.45 \sin(360° \times \frac{284+n}{365}) \quad (3.2.2)$$

Where, n is the day of the year, $1 \leq n \leq 365$

Hour Angle is the angle of radiation due to time of day.

$$\omega = 15° \times (LST - 12) \quad (3.2.3)$$

Where, LST is the local solar time (hours)

$$LST = LT + \frac{TC}{60} \quad (3.2.4)$$

Where, LT is the local standard time (hours)

TC is the time correction (minutes)

$$TC = 4\,(LSTM - Longitude) + EoT \quad (3.2.5)$$

Where, LSTM is the local standard time meridian (°)

EoT is the equation of time (minutes)

$$LSTM = 15° \times \Delta T_{GMT} \text{ --- } (3.2.6)$$

Where, ΔT_{GMT} is the difference of the Local Time from Greenwich Mean Time (hours)

$$EoT = 9.87 \sin(2B) – 7.53 \cos(B) – 1.5 \sin(B) \text{ ----------------------------- } (3.2.7)$$

Where,

$$B = \frac{360}{364}(n\text{-}81) \text{ --- } (3.2.8)$$

Here 'B' is the "Day angle".

3.2.1 Solar Azimuth (β)

The azimuth angle is the angle between true north and the projection of the sunrays on to the horizontal.

$$\beta = \cos^{-1}\left(\frac{\sin(\alpha)\sin(\emptyset) - \sin(\delta)}{\cos(\alpha)\cos(\emptyset)}\right) \text{ ----------------------------------- } (3.2.9)$$

3.3 Procedure for finding the Shadow Length

The solar modules considered are generally placed along the east-west plane facing south. Therefore the projection of the solar radiation on the north-south plane is required.

$$\text{Shadow Length } R = [OO' \times \cos(\Theta)] + [OO' \times \sin(\Theta) \times \frac{\cos\beta}{\tan\alpha}] \text{ ------------------ } (3.2.10)$$

Where, OO' = Module width (mm),

Θ = Tilt angle of panel,

β = Azimuth angle,

α = Altitude angle.

Here,

$$\text{Module row spacing (BM)} = [OO' \times \sin(\Theta) \times \frac{\cos\beta}{\tan\alpha}] \text{ ------------------------- } (3.2.11)$$

CHAPTER 4

DATA TABULATION AND ANALYSIS THE EFFECT OF VARIATION OF SOLAR GEOMETRIC PARAMETERS

4. Data Tabulation And Analysis The Effect Of Variation Of Solar Geometric Parameters

This chapter gives an idea to the reader that how a change of declination angle effects on incident angle, how variation of angle of incidence affects the solar azimuth angle, how variation of hour angle affects the angle of incidence, how R is affected by the change of solar azimuth angle, and few more issues.

Couple of hours just after sunrise and before sunset has less impact on solar PV module in term of power generation; so, for out convenience we have shorter sunshine duration, and all the calculation in this chapter has taken between 9:00 Am and 3:00 PM (6 hours). At this time period the solar irradiation has found better than early morning and late afternoon period. And the effect of shading becomes significant during this time period rather than couple of hours after sunrise and before sunset.

Table-4.1: Variation of B, δ, Equation of time, Time correction with days of the year

Month	Day	Declination (δ) (Degree)	Value of B (Degree)	Equation of Time (Minutes)	Local Standard Time Meridian (Degree)	Time Correction (Minutes)
January	1	-23.0116	-79.1209	-3.6069	90	-5.2569
	5	-22.6466	-75.1648	-5.3637		-7.0137
	10	-22.0396	-70.2198	-7.4229		-9.0729
	15	-21.2695	-65.2747	-9.2868		-10.9368
	20	-20.3419	-60.3297	-10.9144		-12.5644
	25	-19.2636	-55.3846	-12.2717		-13.9217
	30	-18.0428	-50.4396	-13.3320		-14.9820
February	1	-17.5165	-48.4615	-13.6686	90	-15.3186
	5	-16.4023	-44.5055	-14.1873		-15.8373
	10	-14.9009	-39.5604	-14.5426		-16.1926
	15	-13.2892	-34.6154	-14.5736		-16.2236
	20	-11.5790	-29.6703	-14.2905		-15.9405
	25	-9.7832	-24.7253	-13.7120		-15.3620
	28	-8.6700	-21.7582	-13.2336		-14.8836
March	1	-8.2937	-20.7692	-13.0538	90	-14.7038
	5	-6.7649	-16.8132	-12.2400		-13.8900
	10	-4.8097	-11.8681	-11.0335		-12.6835
	15	-2.8189	-6.9231	-9.6563		-11.3063
	20	-0.8072	-1.9780	-7.8437		-9.8047
	25	1.2105	2.9670	-6.2569		-8.2272
	30	3.2192	7.9121	-4.9734		-6.6234
April	1	4.0168	9.8901	-4.0191	90	-5.9856
	5	5.5969	13.8462	-2.7773		-4.7333
	10	7.5338	18.7912	-1.3072		-3.2421
	15	9.4149	23.7363	0.0326		-1.8731
	20	11.2263	28.6813	1.2051		-0.6645
	25	12.9546	33.6264	2.1794		0.3517
	30	14.5870	38.5714	2.9320		1.1501
May	1	14.9009	39.5604	3.0544	90	1.2820
	5	16.1114	43.5165	3.4468		1.7133
	10	17.5165	48.4615	3.7161		2.0320
	15	18.7919	53.4066	3.7405		2.1049
	20	19.9282	58.3516	3.5289		1.9394
	25	20.9170	63.2967	3.0981		1.5507
	30	21.7509	68.2418	2.4723		0.9617
June	1	22.0396	70.2198	2.3264	90	0.6764
	5	22.5385	74.1758	1.6824		0.0324
	10	23.0116	79.1209	0.7645		-0.8855
	15	23.3144	84.0659	-0.2406		-1.8906
	20	23.4446	88.0220	-1.2891		-2.9391
	25	23.4012	92.9670	-2.3356		-3.9856
	30	23.1845	97.9121	-3.3344		-4.9844

Month	Day	Declination (δ) (Degree)	Value of B (Degree)	Equation of Time (Minutes)	Local Standard Time Meridian (Degree)	Time Correction (Minutes)
July	1	23.1205	98.9011	-3.5245	90	-5.1745
	5	22.7962	102.8571	-4.2412		-5.8912
	10	22.2391	107.8022	-5.0142		-6.6642
	15	21.5173	112.7473	-5.6158		-7.2658
	20	20.6363	117.6923	-6.0136		-7.6636
	25	19.6025	122.6374	-6.1814		-7.8314
	30	18.4235	127.5824	-6.1004		-7.7504
August	1	17.9132	129.5604	-5.9275	90	-7.6456
	5	16.8295	133.5165	-5.5497		-7.3099
	10	15.3634	138.4615	-4.8427		-6.6547
	15	13.7836	143.4066	-3.8836		-5.7449
	20	12.1017	148.3516	-2.6901		-4.5965
	25	10.3302	153.2967	-1.2874		-3.2332
	30	8.4822	158.2418	0.2920		-1.6862
September	1	8.1046	160.2198	0.6257	90	-1.0243
	5	6.5714	164.1758	2.0092		0.3592
	10	4.6120	169.1209	3.8203		2.1703
	15	2.6184	174.0659	5.6774		4.0274
	20	0.6054	179.0110	7.5300		5.8800
	25	-1.4120	183.9560	9.3266		7.6766
	30	-3.4190	188.9011	11.0159		9.3659
October	1	-3.8178	189.8901	11.0159	90	9.6865
	5	-5.4007	193.8462	12.2570		10.8988
	10	-7.3424	198.7912	13.6316		12.2294
	15	-9.2297	203.7363	14.7705		13.3168
	20	-11.0487	208.6813	15.6375		14.1256
	25	-12.7859	213.6264	16.2029		14.6278
	30	-14.4284	218.5714	16.4450		14.8032
November	1	-15.3634	220.5495	16.4290	90	14.7790
	5	-16.8295	224.5055	16.2167		14.5667
	10	-18.1710	229.4505	15.6448		13.9948
	15	-19.3780	234.3956	14.7406		13.0906
	20	-20.4415	239.3407	13.5211		11.8711
	25	-21.3537	244.2857	12.0117		10.3617
	30	-21.9699	249.2308	10.2459		8.5959
December	1	-22.1077	250.2198	9.8653	90	8.2153
	5	-22.6981	254.1758	7.8453		6.6137
	10	-23.1205	260.1099	5.6646		4.4612
	15	-23.3717	265.0549	3.3745		2.1888
	20	-23.4498	270.9890	1.0291		-0.1500
	25	-23.3543	274.9451	-1.3164		-2.5000
	30	-23.1533	279.8901	-3.1558		-4.8058

Figure 4.1 shows the variation of Declination angle in Dhaka (Northern hemisphere) of any year. It also says that in summer in northern hemisphere the declination angle is higher that means the sun altitude angle is higher and the zenith angle is lower and eventually the shadow of any object is lower than winter or spring time.

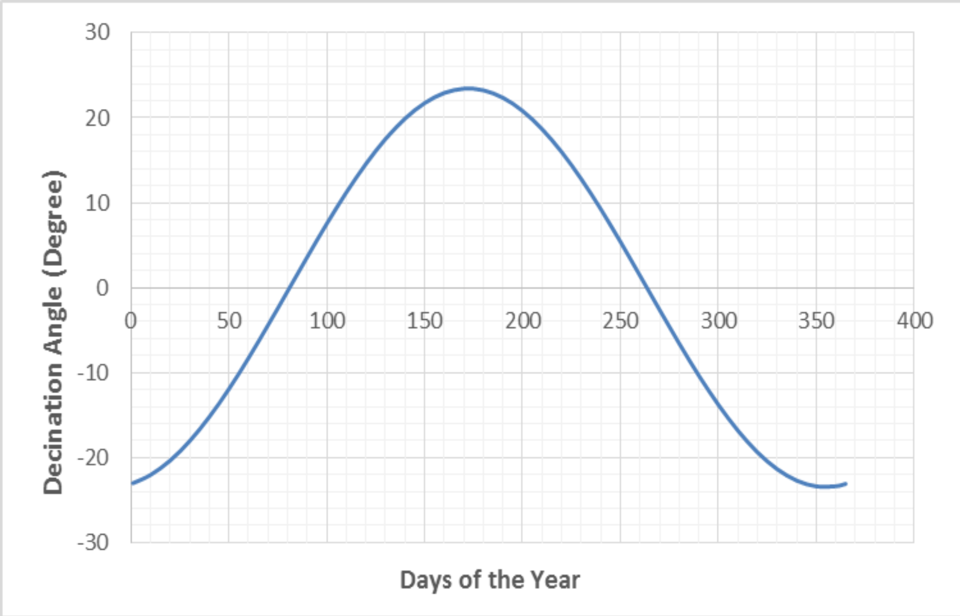

Figure 4.1 Declination angle variation over the year in Dhaka (Northern Hemisphere)

Figure 4.2 shows trends of "B" over the year. But the value of "B" over the year is fixed in anywhere around the world. And from the figure it can be seen that the change in the value of B is linear with the number of days in a year.

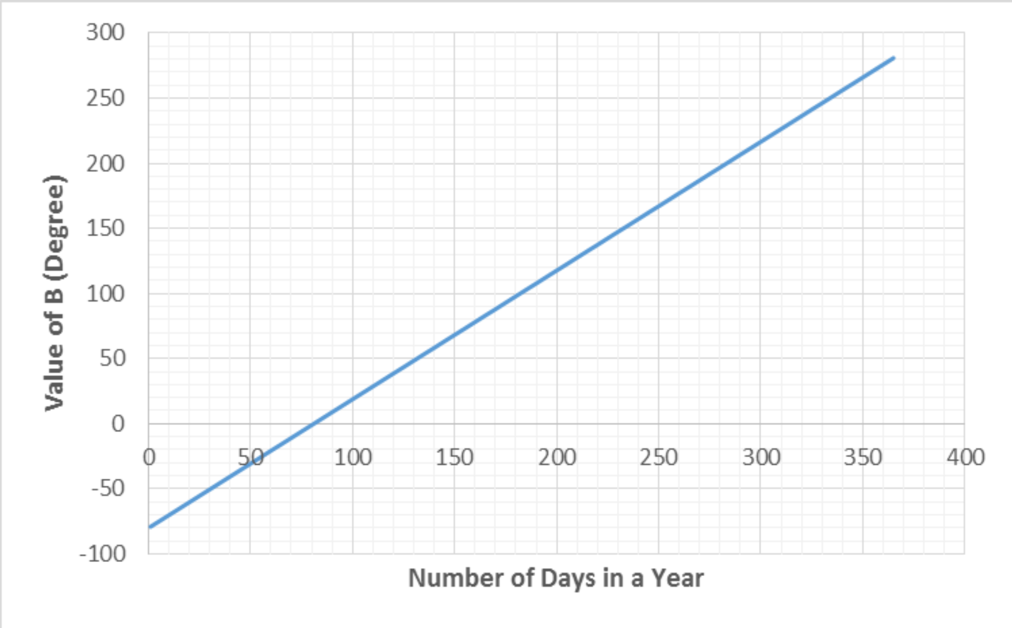

Figure 4.2 Angle "B" variation over the year in whole world.

Figure 3.5 shows trends of annual variation of the "Equation of Time". Here we can see that, the values are changing continuously over the year and shifting from negative to positive value and vice-versa four times. And the maximum positive value is 1st November and maximum negative value is 14th February.

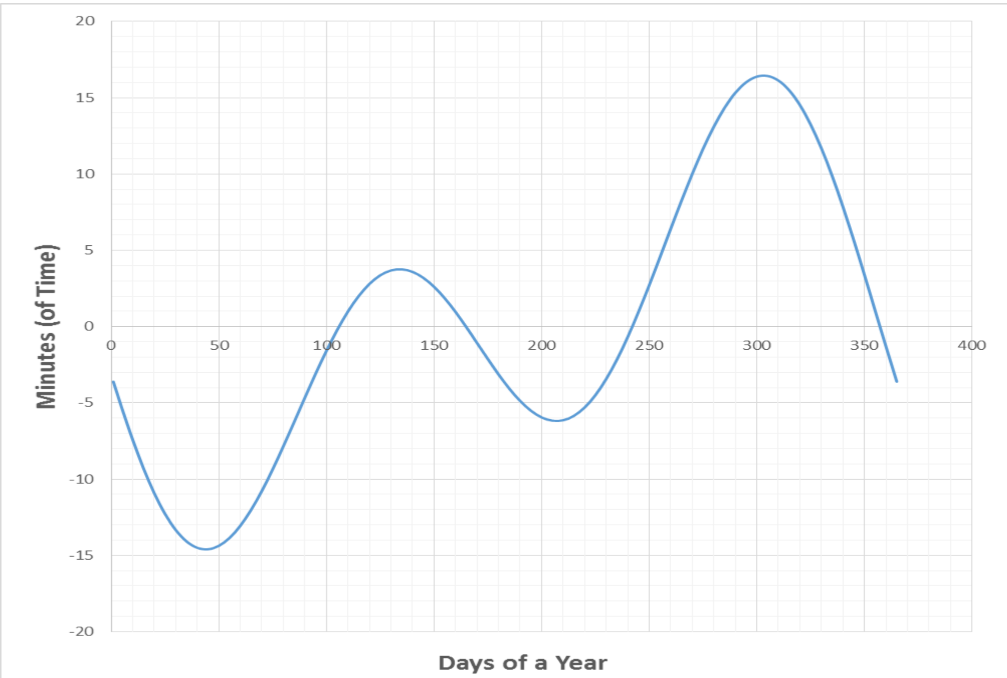

Figure 4.3: Trends in the "Equation of Time (EQT)" over a year.

Table 4.2: Variation of solar azimuth angle, β with the variation of hour angle and declination angle

Month	Day	Declination, δ	Hour angle, ω		Azimuth Angle
			Solar time	Local time	
January	1	-23.0116	8:55 AM	9:00 AM	
			11:55 AM	12:00 PM	1.6583
			2:55 PM	3:00 PM	45.4263
January	15	-21.2695	8:49 AM	9:00 AM	49.6971
			11:49 AM	12:00 PM	3.5949
			2:49 PM	3:00 PM	45.7625
February	1	-17.5165	8:45 AM	9:00 AM	53.3654
			11:45 AM	12:00 PM	5.4219
			2:45 PM	3:00 PM	47.8125
February	15	-13.2892	8:44 AM	9:00 AM	56.7842
			11:44 AM	12:00 PM	5.4310
			2:44 AM	3:00 PM	51.7372
March	1	-8.2937	8:45 AM	9:00 AM	61.9626
			11:45 AM	12:00 PM	6.8188
			2:45 PM	3:00 PM	56.5303
March	15	-2.8189	8:49 AM	9:00 AM	67.2744
			11:49 AM	12:00 PM	6.2049
			2:49 PM	3:00 PM	49.0301
April	1	4.0168	8:54 AM	9:00 AM	73.1734
			11:54 AM	12:00 PM	4.5505
			2:54 PM	3:00 PM	71.0992
April	15	9.4149	8:58 AM	9:00 AM	79.5543
			11:58 AM	12:00 PM	1.8515
			2:58 PM	3:00 PM	79.0185
May	1	14.9009	9:01 AM	9:00 AM	86.0314
			12:01 PM	12:00 PM	1.7390
			3:01 PM	3:00 PM	86.3014
May	15	18.7919	9:02 AM	9:00 AM	91.8993
			12:02 PM	12:00 PM	5.6809
			3:02 PM	3:00 PM	92.2854
June	1	22.0396	9:01 AM	9:00 AM	96.3501
			12:01 PM	12:00 PM	6.1921
			3:01 PM	3:00 PM	96.4881
June	15	23.3144	8:58 AM	9:00 AM	98.7822
			11:58 AM	12:00 PM	35.5347
			2:58 PM	3:00 PM	98.5753
July	1	23.1205	8:55 AM	9:00 AM	98.4760
			11:55 AM	12:00 PM	55.1698
			2:55 PM	3:00 PM	97.7439

July	15	21.5173	8:53AM	9:00 AM	96.8222
			11:53 AM	12:00 PM	38.0460
			2:53 PM	3:00 PM	95.7851
August	1	17.9132	8:52 AM	9:00 AM	92.6284
			11:52 AM	12:00 PM	19.8088
			2:52 PM	3:00 PM	91.1872
August	15	13.7836	8:54 AM	9:00 AM	84.3534
			11:54 AM	12:00 PM	6.4532
			2:54 PM	3:00 PM	83.0629
September	1	8.1046	8:58 AM	9:00 AM	76.7709
			11:58 AM	12:00 PM	0.5921
			2:58 PM	3:00 PM	76.5634
September	15	2.6184	9:05 AM	9:00 AM	68.7789
			12:05 PM	12:00 PM	3.1277
			3:05 PM	3:00 PM	70.4044
October	1	-3.8178	9:10 AM	9:00 AM	61.1970
			12:10 PM	12:00 PM	5.2233
			3:10 PM	3:00 PM	64.8252
October	15	-9.2297	9:14 AM	9:00 AM	54.7675
			12:14 PM	12:00 PM	5.9754
			3:14 PM	3:00 PM	59.8376
November	1	-15.3634	9:15 AM	9:00 AM	49.9606
			12:15 PM	12:00 PM	5.6249
			3:15 PM	3:00 PM	55.4190
November	15	-19.3780	9:13 AM	9:00 AM	46.9317
			12:13 PM	12:00 PM	4.4281
			3:13 PM	3:00 PM	51.6112
December	1	-22.1077	9:08 AM	9:00 AM	45.6018
			12:08 PM	12:00 PM	2.6469
			3:00 PM	3:00 PM	48.5402
December	15	-23.3717	9:02 AM	9:00 AM	45.7779
			12:02 PM	12:00 PM	0.5457
			3:02 PM	3:00 PM	46.3884

From figure 4.4 the following figure, we can see that at 12:00 pm over the year, the value of solar azimuth angle was the minimum. And at 10:00 AM and 3:00 PM the value of solar azimuth angle was the maximum. And we can also see that at time 10:00 AM, 11:00 AM, 1:00 PM, 2:00 PM, 3:00 PM, the value of azimuth changes in an uniform way, but at 12:00 PM the value doesn't change that uniformly.

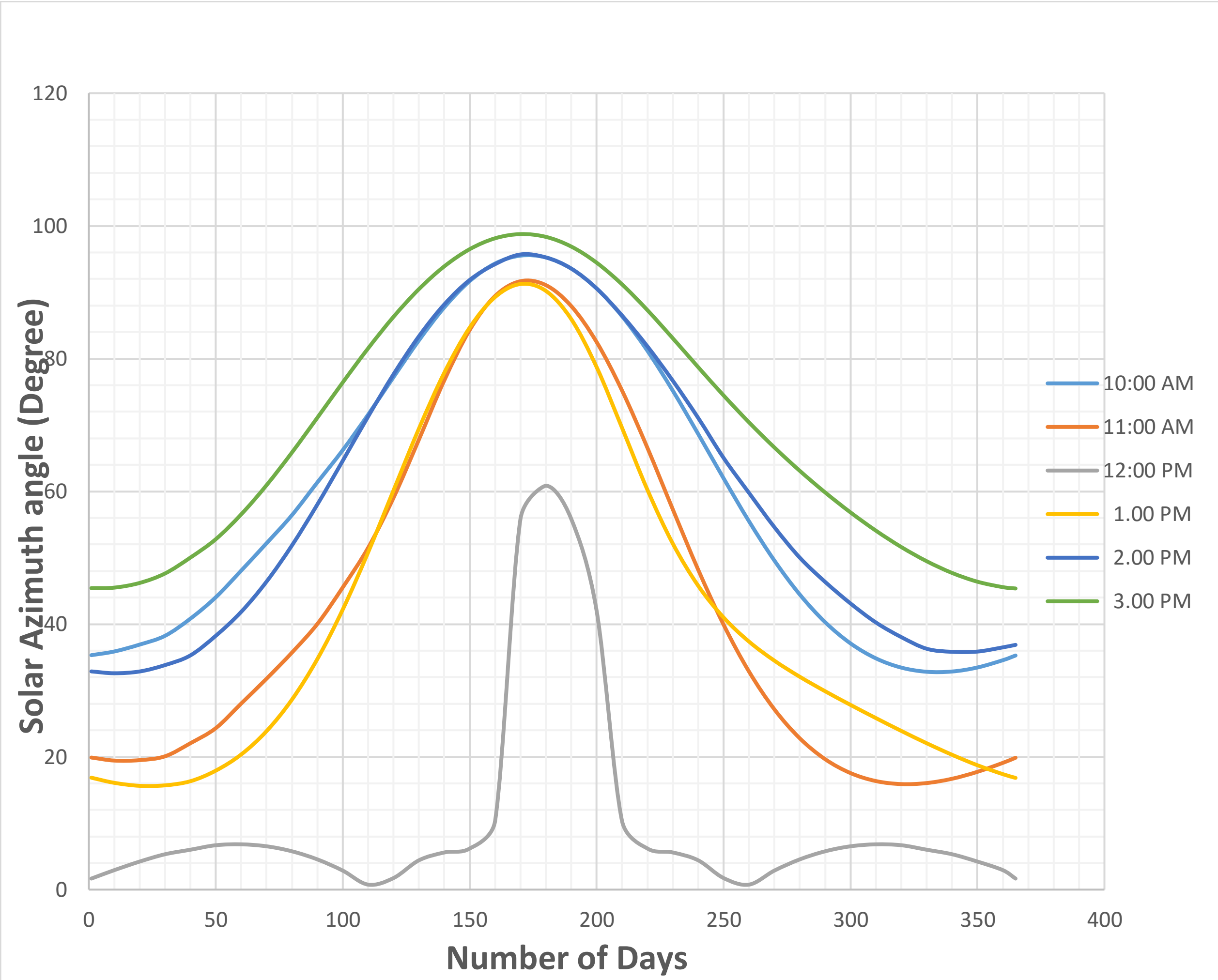

Figure 4.4: Trends on Solar Azimuth Angle at specific time over a year.

Table 4.3: Variation of solar Elevation angle, β with the variation of hour angle and declination angle.

Month	Day	Declination, δ	Hour angle, ω		Solar Elevation Angle
			Solar time	Local time	
January	1	-23.0116	8:55 AM	9:00 AM	25.0758
			11:55 AM	12:00 PM	43.1607
			2:55 PM	3:00 PM	26.8159
January	15	-21.2695	8:49 AM	9:00 AM	25.2749
			11:49 AM	12:00 PM	44.8417
			2:49 PM	3:00 PM	28.9787
February	1	-17.5165	8:45 AM	9:00 AM	26.7865
			11:45 AM	12:00 PM	48.2433
			2:45 PM	3:00 PM	32.1463
February	15	-13.2892	8:44 AM	9:00 AM	29.6839
			11:44 AM	12:00 PM	52.4222
			2:44 AM	3:00 PM	34.7432
March	1	-8.2937	8:45 AM	9:00 AM	32.6535
			11:45 AM	12:00 PM	57.6957
			2:45 PM	3:00 PM	38.4370
March	15	-2.8189	8:49 AM	9:00 AM	36.6921
			11:49 AM	12:00 PM	63.6355
			2:49 PM	3:00 PM	41.2713
April	1	4.0168	8:54 AM	9:00 AM	40.7762
			11:54 AM	12:00 PM	69.7509
			2:54 PM	3:00 PM	43.5218
April	15	9.4149	8:58 AM	9:00 AM	44.3480
			11:58 AM	12:00 PM	75.5977
			2:58 PM	3:00 PM	45.1894
May	1	14.9009	9:01 AM	9:00 AM	46.9605
			12:01 PM	12:00 PM	80.7727
			3:01 PM	3:00 PM	46.4347
May	15	18.7919	9:02 AM	9:00 AM	48.4250
			12:02 PM	12:00 PM	84.9577
			3:02 PM	3:00 PM	47.4623
June	1	22.0396	9:01 AM	9:00 AM	48.8491
			12:01 PM	12:00 PM	87.9287
			3:01 PM	3:00 PM	48.4127
June	15	23.3144	8:58 AM	9:00 AM	48.5381
			11:58 AM	12:00 PM	89.3338
			2:58 PM	3:00 PM	49.3005
July	1	23.1205	8:55 AM	9:00 AM	47.8324
			11:55 AM	12:00 PM	88.7639
			2:55 PM	3:00 PM	49.9978

July	15	21.5173	8:53AM	9:00 AM	46.9888
			11:53 AM	12:00 PM	87.3010
			2:53 PM	3:00 PM	50.2433
August	1	17.9132	8:52 AM	9:00 AM	46.1321
			11:52 AM	12:00 PM	84.5495
			2:52 PM	3:00 PM	49.6926
August	15	13.7836	8:54 AM	9:00 AM	45.2438
			11:54 AM	12:00 PM	80.5071
			2:54 PM	3:00 PM	48.0445
September	1	8.1046	8:58 AM	9:00 AM	43.7326
			11:58 AM	12:00 PM	73.5313
			2:58 PM	3:00 PM	76.5634
September	15	2.6184	9:05 AM	9:00 AM	44.0371
			12:05 PM	12:00 PM	67.5719
			3:05 PM	3:00 PM	40.0215
October	1	-3.8178	9:10 AM	9:00 AM	39.7833
			12:10 PM	12:00 PM	61.4734
			3:10 PM	3:00 PM	64.8252
October	15	-9.2297	9:14 AM	9:00 AM	35.7056
			12:14 PM	12:00 PM	55.6963
			3:14 PM	3:00 PM	31.6656
November	1	-15.3634	9:15 AM	9:00 AM	30.6382
			12:15 PM	12:00 PM	46.6979
			3:15 PM	3:00 PM	26.1747
November	15	-19.3780	9:13 AM	9:00 AM	46.9317
			12:13 PM	12:00 PM	4.4281
			3:13 PM	3:00 PM	51.6112
December	1	-22.1077	9:08 AM	9:00 AM	27.9380
			12:08 PM	12:00 PM	44.0386
			3:00 PM	3:00 PM	25.1863
December	15	-23.3717	9:02 AM	9:00 AM	25.9852
			12:02 PM	12:00 PM	42.8161
			3:02 PM	3:00 PM	25.4178

From figure 4.5, the following figure we can see that on 21st June the value of solar elevation angle is higher and on 21st December and 21st January, the value of solar elevation angle is comparatively lowest and the value of solar elevation angle on other days of a year remain in between these values.

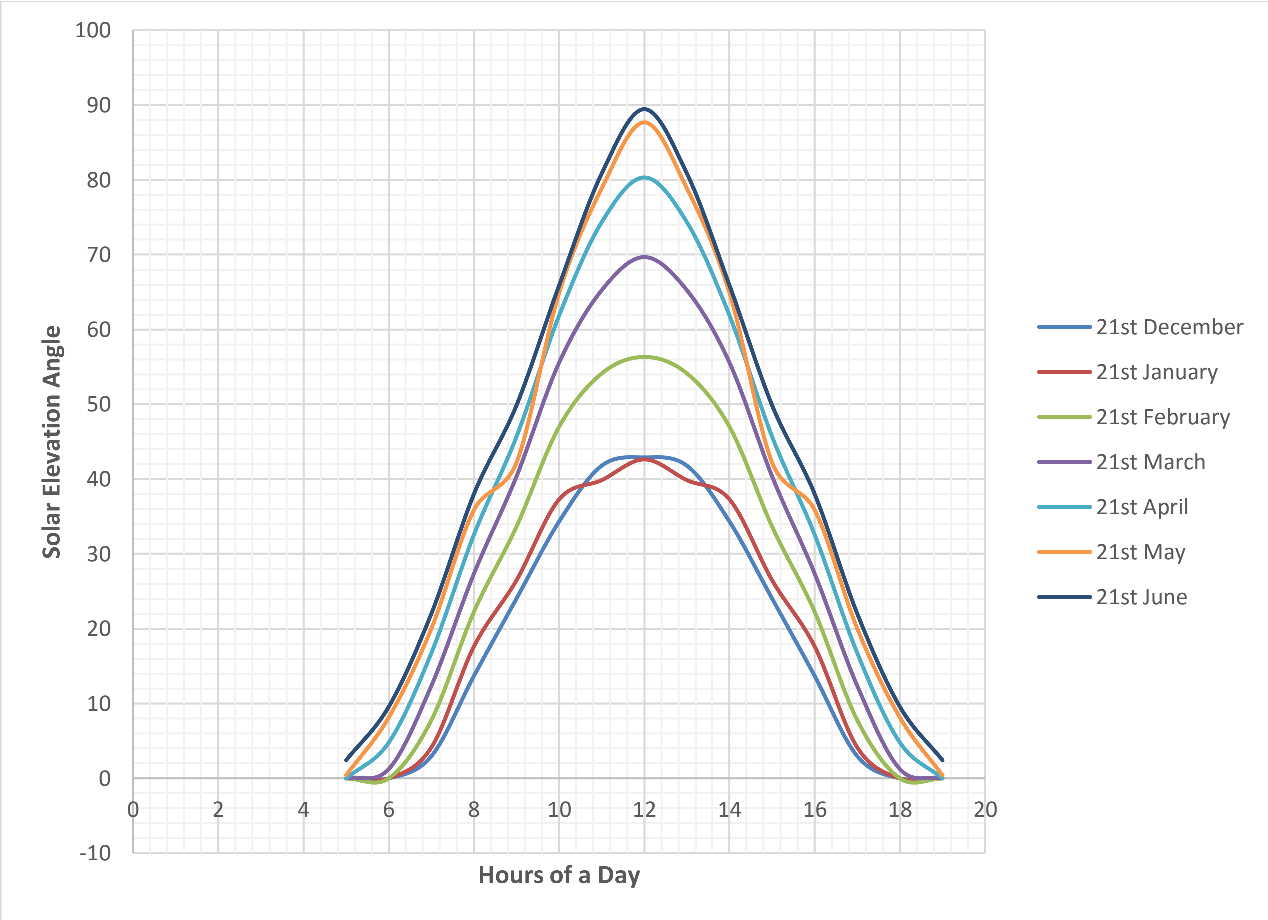

Figure 4.5: Trends on Solar Elevation Angle over specific days of a year.

Table 4.4: Variation of Shadow length and Row spacing with the variation of Hour angle and Declination angle over the year.

Month	Day	Declination, δ	Hour angle, ω		Shadow length (mm)	Row Spacing(mm)
			Solar time	Local time		
January	1	-23.0116	8:55 AM	9:00 AM	2397.220	932.167
			11:55 AM	12:00 PM	2160.573	695.523
			2:55 PM	3:00 PM	2310.897	845.847
January	15	-21.2695	8:49 AM	9:00 AM	2346.087	881.037
			11:49 AM	12:00 PM	2045.505	580.455
			2:49 PM	3:00 PM	2275.213	810.163
February	1	-17.5165	8:45 AM	9:00 AM	2234.245	769.195
			11:45 AM	12:00 PM	1940.882	475.832
			2:45 PM	3:00 PM	2160.477	695.427
February	15	-13.2892	8:44 AM	9:00 AM	2110.108	645.058
			11:44 AM	12:00 PM	1870.695	405.645
			2:44 AM	3:00 PM	2039.310	574.260
March	1	-8.2937	8:45 AM	9:00 AM	1973.792	508.742
			11:45 AM	12:00 PM	1813.919	348.869
			2:45 PM	3:00 PM	1896.524	431.474
March	15	-2.8189	8:49 AM	9:00 AM	1840.454	375.404
			11:49 AM	12:00 PM	1755.925	290.875
			2:49 PM	3:00 PM	1785.54	320.49
April	1	4.0168	8:54 AM	9:00 AM	1675.325	210.275
			11:54 AM	12:00 PM	1691.533	226.483
			2:54 PM	3:00 PM	1674.425	209.375
April	15	9.4149	8:58 AM	9:00 AM	1584.352	119.302
			11:58 AM	12:00 PM	1650.144	185.094
			2:58 PM	3:00 PM	1586.732	121.682
May	1	14.9009	9:01 AM	9:00 AM	1506.615	41.565
			12:01 PM	12:00 PM	1595.496	130.446
			3:01 PM	3:00 PM	1504.539	39.489
May	15	18.7919	9:02 AM	9:00 AM	1483.958	18.908
			12:02 PM	12:00 PM	1560.518	95.468
			3:02 PM	3:00 PM	1488.589	23.539
June	1	22.0396	9:01 AM	9:00 AM	1527.242	62.192
			12:01 PM	12:00 PM	1515.203	50.153
			3:01 PM	3:00 PM	1529.557	64.507
June	15	23.3144	8:58 AM	9:00 AM	1551.81	86.76
			11:58 AM	12:00 PM	1490.16	25.11
			2:58 PM	3:00 PM	1547.565	82.515
July	1	23.1205	8:55 AM	9:00 AM	1555.54	90.49
			11:55 AM	12:00 PM	1471.203	6.153
			2:55 PM	3:00 PM	1543.384	78.334

July	15	21.5173	8:53AM	9:00 AM	1501.709	36.659
			11:53 AM	12:00 PM	1505.203	40.153
			2:53 PM	3:00 PM	1480.421	15.371
August	1	17.9132	8:52 AM	9:00 AM	1512.449	47.399
			11:52 AM	12:00 PM	1540.518	75.468
			2:52 PM	3:00 PM	1529.042	63.992
August	15	13.7836	8:54 AM	9:00 AM	1709.864	244.814
			11:54 AM	12:00 PM	1595.496	130.446
			2:54 PM	3:00 PM	1684.075	219.025
September	1	8.1046	8:58 AM	9:00 AM	1852.118	387.068
			11:58 AM	12:00 PM	1640.144	175.094
			2:58 PM	3:00 PM	1796.524	331.474
September	15	2.6184	9:05 AM	9:00 AM	1998.325	533.275
			12:05 PM	12:00 PM	1691.533	226.483
			3:05 PM	3:00 PM	1934.057	469.007
October	1	-3.8178	9:10 AM	9:00 AM	2125.555	660.505
			12:10 PM	12:00 PM	1750.925	285.875
			3:10 PM	3:00 PM	2083.944	618.894
October	15	-9.2297	9:14 AM	9:00 AM	2240.944	775.894
			12:14 PM	12:00 PM	1813.919	348.869
			3:14 PM	3:00 PM	2210.669	745.619
November	1	- 15.3634	9:15 AM	9:00 AM	2306.526	841.476
			12:15 PM	12:00 PM	1870.695	405.645
			3:15 PM	3:00 PM	2297.593	832.543
November	15	- 19.3780	9:13 AM	9:00 AM	2363.545	898.495
			12:13 PM	12:00 PM	1945.882	480.832
			3:13 PM	3:00 PM	2370.527	905.477
December	1	- 22.1077	9:08 AM	9:00 AM	2395.319	930.269
			12:08 PM	12:00 PM	2045.505	580.455
			3:00 PM	3:00 PM	2398.568	933.518
December	15	- 23.3717	9:02 AM	9:00 AM	2400.433	935.383
			12:02 PM	12:00 PM	2152.374	687.324
			3:02 PM	3:00 PM	2399.944	934.894

From figure 4.6, the following figure we can see the trend of the variation of shadow length and module row spacing at LST 09:00 AM over the year. Here the shadow length and module row is maximum on January and December and it is very low comparatively April to July. From 10th April to August 28, the value of shadow length and module row spacing is comparatively less.

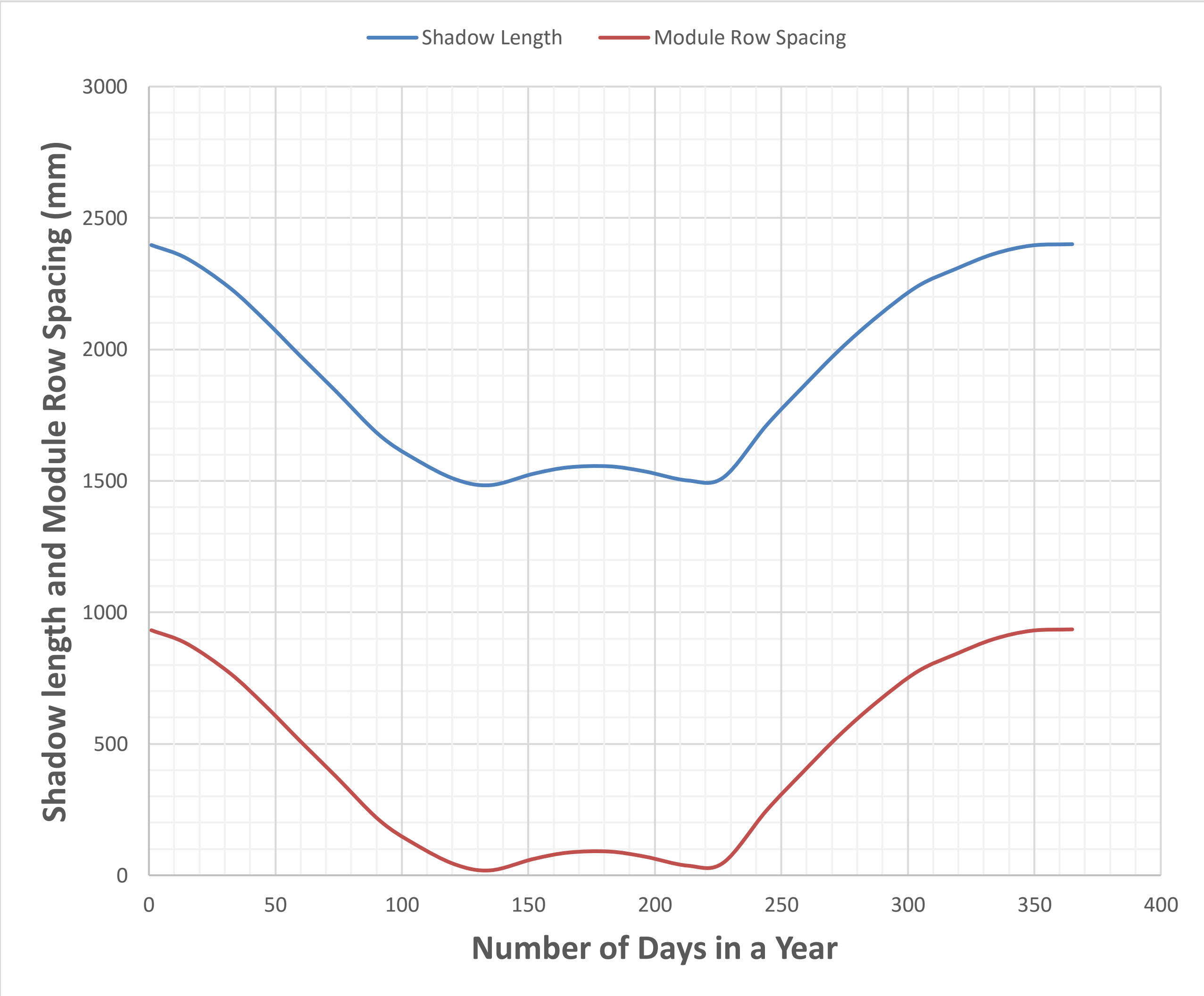

Figure 4.6: Shadow Length and Module Row Spacing at LST 09:00 in a year.

From the figure 4.7, we can see the variation of shadow length and module row spacing at LST 12:00 PM over the year. Here the shadow length and module row is maximum on January and December and it is very low comparatively April to July. From 10th April to August 28, the value of shadow length and module row spacing is comparatively less.

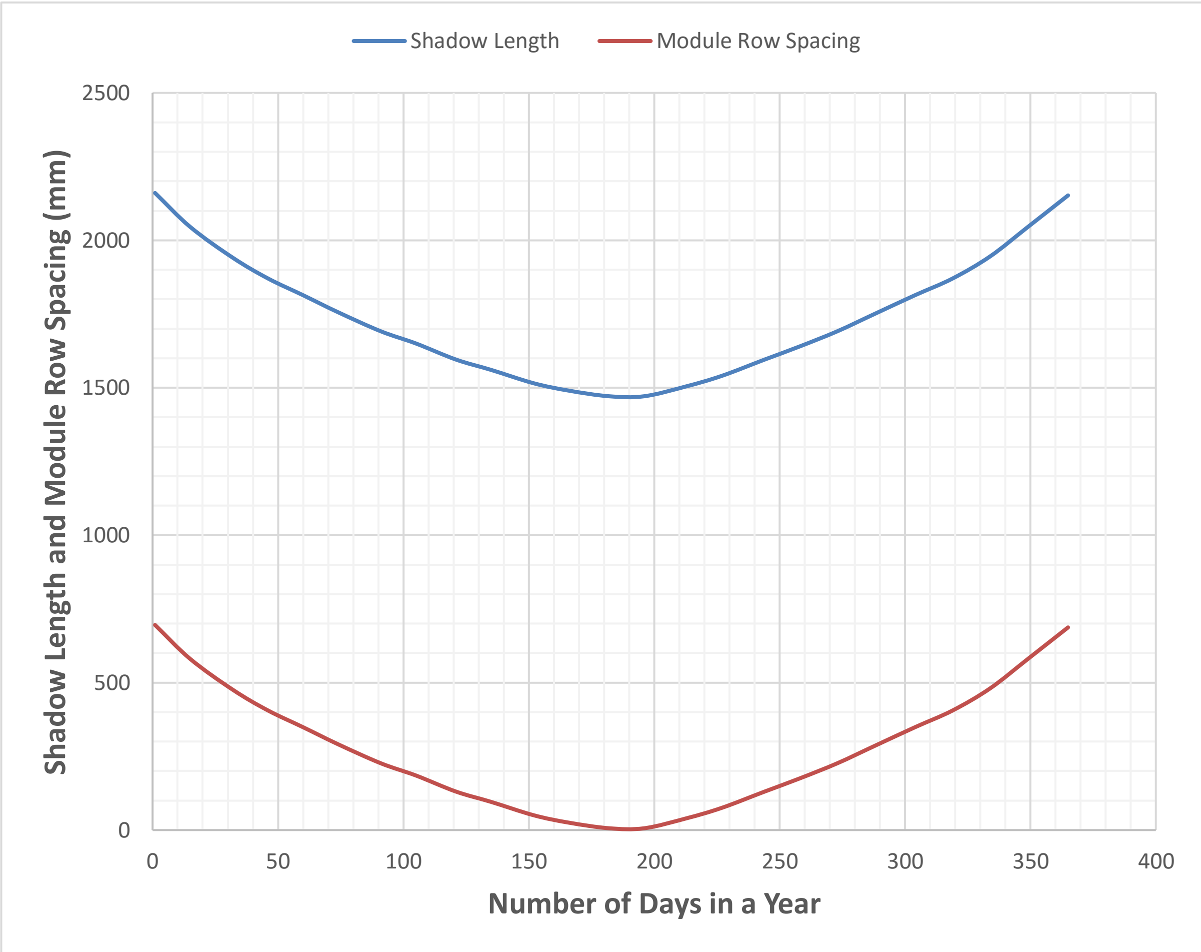

Figure 4.7: Shadow Length and Module Row Spacing at LST 12:00 over the year.

From the figure 4.8, we can see the variation of shadow length and module row spacing at LST 3:00 PM over the year. Here the shadow length and module row is maximum on January and December and it is very low comparatively April to July. From 10th April to August 28, the value of shadow length and module row spacing is comparatively less.

Figure 4.8: Trend in Shadow Length and Module Row Spacing at LST 3:00 PM in a Year.

CHAPTER 5

METHODOLOGY FOR SELECTION OF OPTIMAL SHADOW LENGTH FOR CHOOSING MINIMUM MODULE ROW SPACING

5 Methodology For Selection Of Optimal Shadow Length For Choosing Minimum Module Row Spacing

Shadow length at the time of sunset and sunrise is quite high as altitude is very low. Moreover, the irradiation is comparatively very less, so consequently PV generation is minimal. Therefore, while calculating the maximum shadow length for finding the minimum spacing between consecutive parallel rows of solar modules, these values should be avoided. For this purpose total sunshine hours need to be considered.

In the following table, on a particular day in Dhaka, The sun rises at 6 AM LST and sun sets at 6:00 PM LST. Then there are 12 sunshine hours of that day. Solar noon occurs at 12:00 PM LST when altitude in maximum. From 12 noon to 6 am in the morning as well as 12 noon to 6 pm in the evening the altitude gradually decreases and thus the shadow length increases. So, in this case 100% sunshine hours are considered, which means calculation of shadow length is done considered, which means calculation of shadow length is done for all the 12 hours of that day from sunrise to sunset. If for this very day 50% sunshine hors are considered, then 6 hours are considered in total for shadow calculations – 3 hours before solar noon and 3 hours after solar noon. It is worth to mention that, all the calculations are done on the hourly basis and if for 20% sunshine hours the considered time is 2.4 hours then the time is rounded to the nearest integer i.e., 2 hours and the calculations are done accordingly.

Table 5.1: Trends of Percentage sunshine hour with duration and time span in consideration with the solar noon of 12:00 PM

Percentage of sunshine hour	Duration Hours	Time span
5%	0.5	11:45 AM-12.15 PM
10%	1	11:30 AM-12:30 PM
15%	1.5	11:15 AM-12:45 PM
20%	2	11:00 AM-1:00 PM
25%	3	10:30 AM-1:30 PM
30%	4	10:00 AM-2:00 PM
35%	4.5	9:45 AM-2:15 PM
40%	5	9:30 AM – 2:30 PM
45%	5.5	9:15 AM – 2:45 PM
50%	6	9:00 AM – 3:00 PM
55%	6.5	8:45 AM – 3:15 PM
60%	7	8:30 AM – 3:30 PM
65%	7.5	8:15 AM – 3:45 PM
70%	8	8:00 AM – 4:00 PM
75%	8.5	7:45 AM – 4:15 PM
80%	9	7:30 AM – 4:30 PM
85%	10	7:00 AM – 5:00 PM
90%	11	6:30 AM – 5:30 PM
95%	11.5	6:15 AM – 5:45 PM
100%	12	6:00 AM – 6:00 PM

Now with the help of information from the table, we have found out the shadow length and corresponding module row spacing at different percentage of sunshine hour. And from those information we have selected a maximum shadow length for which we can have minimum module row spacing so that, maximum power can be generated by minimizing the shading effect of front panels.

Table 5.2: Selection of Maximum shadow length and module row spacing for specific percentage of sunshine hour.

Percentage of sunshine hour	Duration	Time span	Maximum shadow length (mm)	Module Row Spacing (mm)
50%	6	9:00 AM – 3:00 PM	2399.944	934.894
55%	6.5	8:45 AM – 3:15 PM	2514.254	1049.204
60%	7	8:30 AM – 3:30 PM	2657.215	1192.165
65%	7.5	8:15 AM – 3:45 PM	2745.254	1280.204
70%	8	8:00 AM – 4:00 PM	2870.761	1405.711

From the table, we can see that for sunshine hour of 50%, that is the time span of 9:00 AM to 3:00 PM, the maximum shadow length is 2399.944 mm and module row spacing is 934.894 mm. But for more percentage sunshine hour the shadow length is increasing excessively so does the module row spacing which will cost a greater area for installation but will result in very minimal increase of power.

So Maximum Shadow Length of 2399.944 mm and Minimum Module Row Spacing of 934.894 mm is chosen for Dhaka city for a percentage of sunshine hour of 50% and time span from 9:00 AM to 3:00 pm.

Now, in next Chapter, we will see how SUN-PATH diagram will help us to reduce the module row spacing so that to produce maximum possible power using less space for solar panel packing.

CHAPTER 6

Methodology For Obtaining Minimum Module Row Spacing From Sun-Path Diagram For A Latitude

6. Methodology For Obtaining Minimum Module Row Spacing From Sun-Path Diagram For A Latitude

6.1 Sun Path Diagram

Sun path diagrams are a convenient way of representing the annual changes in the path of the Sun through the sky on a single 2D diagram. Their most immediate use is that the solar azimuth and altitude can be read off directly for any time of the day and month of the year. They also provide a unique summary of solar position that the architect can refer to when considering shading requirements and design options. There are quite a few different types of sun-path diagrams, however, we will only examine two main forms.

There are different types of sun-path diagram. We have used cylindrical diagrams.

6.2 Cylindrical Diagram

A cylindrical projection is simply a 2D graph of the Sun position in Cartesian coordinates. The azimuth is plotted along the horizontal axis whilst the altitude is plotted vertically. Reading off positions is simply a matter of reading off the two axis, as shown below.

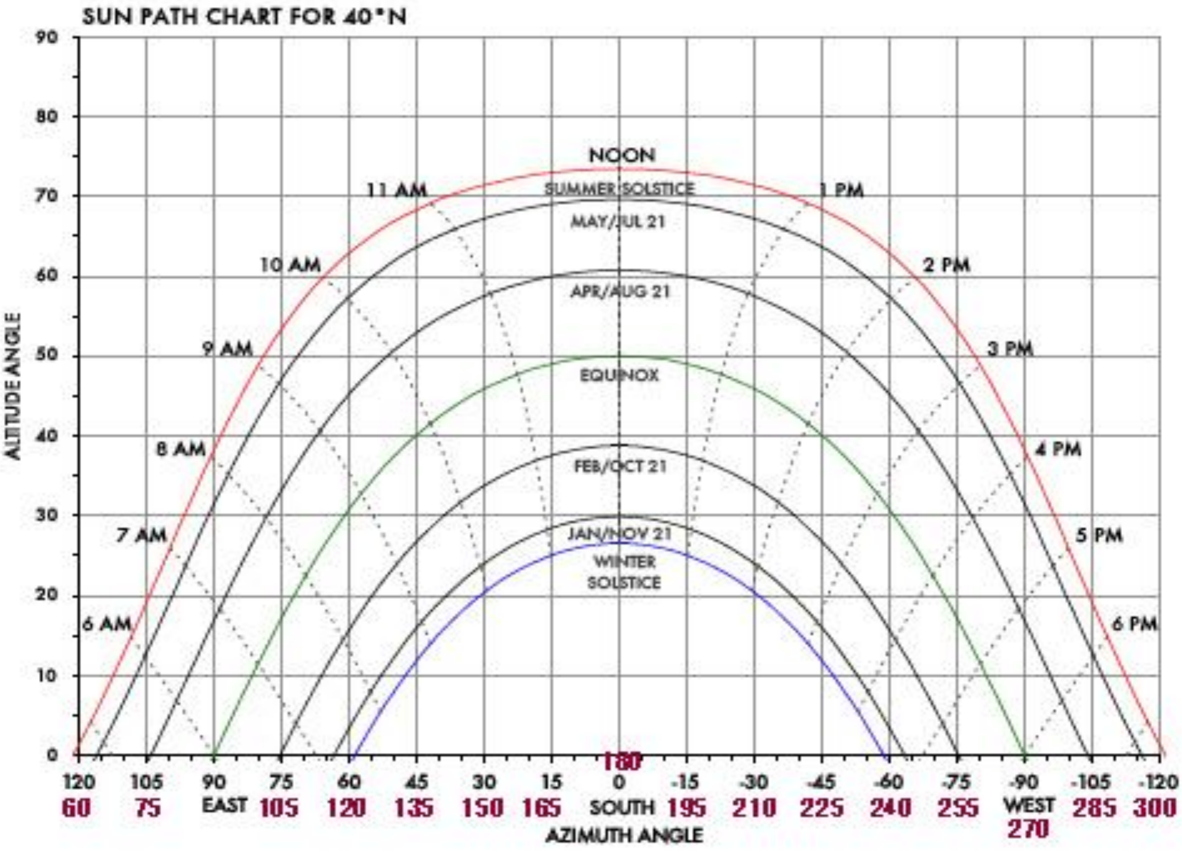

Figure 6.1: Cylindrical sun-path diagram for a latitude of 40°N.

We have drawn a sun-path diagram for Dhaka city which latitude is 23.8103°

From figure 6.2, (sun-path diagram) we can have azimuth correction angle for which we can find out the minimum module row spacing which will increase the module arrangement compactness even better than the findings of previous chapter.

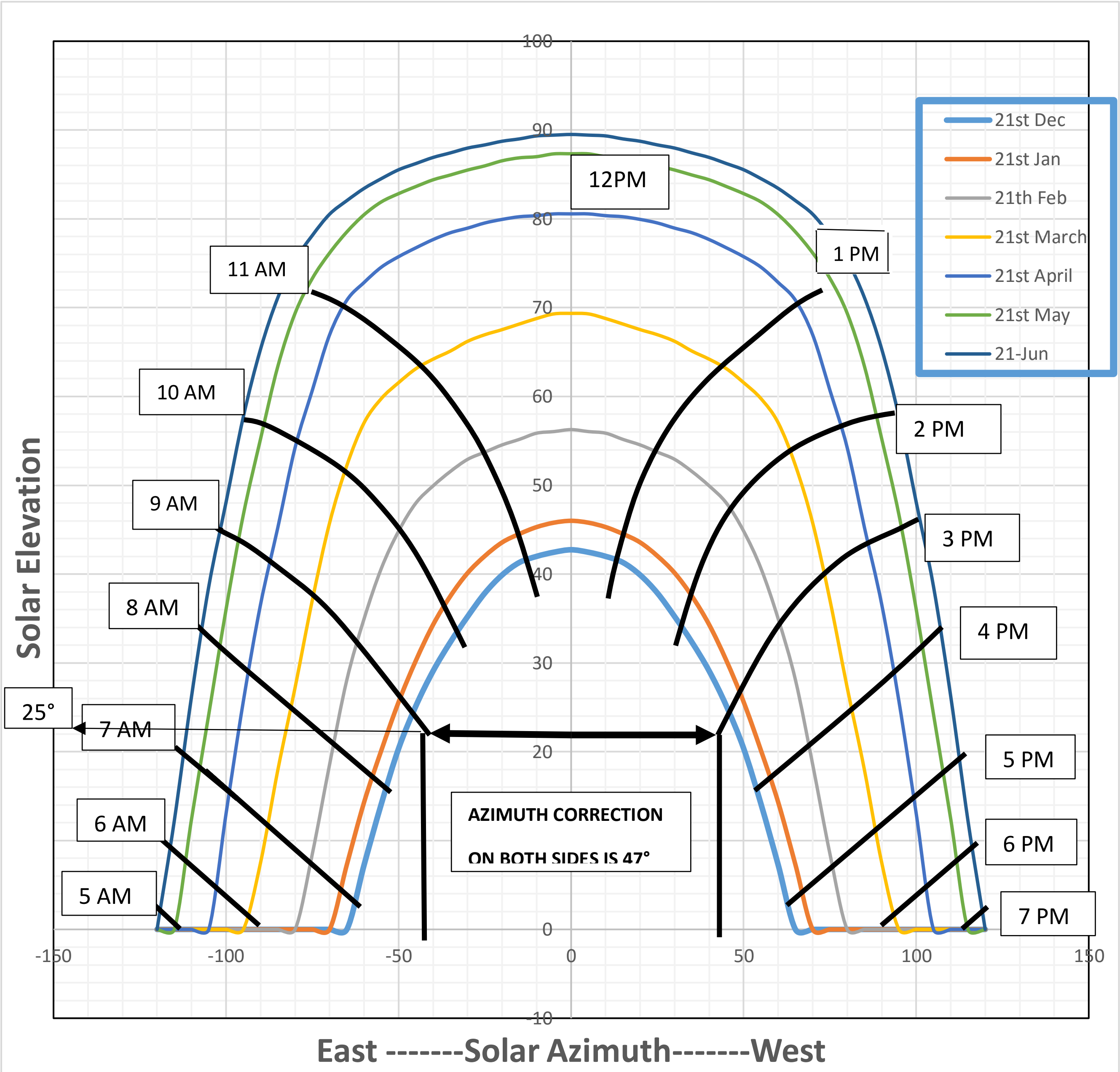

Figure 6.2 Sun-path diagram of Dhaka city, Bangladesh

6.3 Calculation of minimum module row spacing from the sun-path diagram

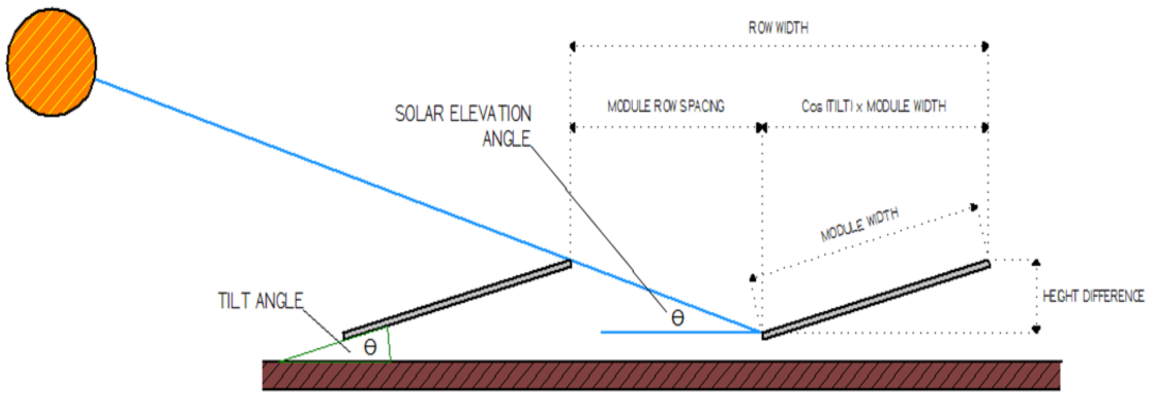

Figure 6.3: **Module row spacing between successive rows.**

When the sunshine duration is considered 50%, time span from 9:00 AM to 3:00 PM

Here, Azimuth correction = 47°

Solar Elevation angle = 25°

The first step in calculating the inter-row spacing for our modules is to calculate the height difference from the back of the module to the surface. To do that, we have to follow this calculation below.

Height difference between the top of a panel and the bottom of next panel

= Sin (Tilt angle) × Module Width

= Sin 23.8103 × 1600

= 645.936 mm

Module row spacing = Height difference/ tan (solar elevation angle)

= 645.936/tan(25°)

= 1385.214 mm.

Minimum module row spacing = Module row spacing × cos (azimuth correction angle)

= 1385.214 × cos (47°)

= 944.714 mm.

Table 6.1: Comparison between the value of minimum module row spacing from the mathematical model previously calculated and that from the sun-path diagram.

Percentage of sunshine hour	Duration	Time span	Module Row Spacing from Mathematical Model (mm)	Module Row Spacing from Sun-Path Diagram (mm)	Percentage deviation of both values
50%	6	9:00 AM – 3:00 PM	934.894	944.714	1.05%
55%	6.5	8:45 AM – 3:15 PM	1049.204	1055.365	0.587%
60%	7	8:30 AM – 3:30 PM	1192.165	1201.528	0.785%
65%	7.5	8:15 AM – 3:45 PM	1280.204	1289.214	0.704%
70%	8	8:00 AM – 4:00 PM	1405.711	1417.253	0.821%

From the table we can come to a conclusion that we can choose minimum module row spacing from any of the method viz. Mathematical model or from sun-path diagram as the reading is almost same in both the cases.

So, finally it is inferred that, minimum module row spacing of 944.714 mm is chosen for a percentage sunshine hour of 50% and time span from 9:00 AM to 3:00 PM.

CHAPTER 7

METHODOLOGY FOR OBTAINING MAXIMUM POWER GENERATION USING OPTIMAL ROW SPACING

7 Methodology For Obtaining Maximum Power Generation Using Optimal Row Spacing

One of the challenges for setting up of solar panel is to maximizing the power generation by compactly arrange the solar modules. But as we have discussed earlier that compact arrangement will increase the shading affect. That's why we have calculated the minimum module row spacing which will lessen the affect of shadow.

Now, we will focus, how incorporation of minimum module row spacing can lead to arrangement will increase more module in limited spaces and so does the power generation.

Let us consider a 30 meter by 29 meter spaces at rooftop of a building for the setup of solar module.

Length of the space = 30 m.

Width of the space = 29 m.

Therefore, Number of panel of width of 1600 mm and length 30 m can be set up is,

= 10

2 square meter panel x 1000 = 2000 x 0.20 (20% efficiency panel) = 400. 400 x 5 hours of sun hours = 2000 Watt hours per day. (Adopted from – The eco expert- http://www.theecoexperts.co.uk/how-much-electricity-can-i-generate-solar-panels)

But if we incorporate minimum module row spacing than we can set up modules of similar dimension of

= 12

Power generation by 10 panel throughout the year will be

$= (48\times10)\ m^2 \times 1000\ W/m^2 \times 0.20\ (\text{Efficiency}) \times 5\ \text{hours} \times 365\ \text{days}$

$= 1.752 \times 10^8$ Watt hours.

= 175200 KW-hours

If we consider 1 KW-hour price is 5.00 BDT, then the cost of this electricity will be

= 8,76,000 BDT.

Similarly power generation by 12 panel throughout the year will be

= (48×12)×1000×0.20×5×365

= 2.1024 × 10^8 Watt hours.

= 2,10,240 KW-hours

= 10,51,200 BDT.

Money saved throughout the year = (10,51,200 – 8,76,000) BDT

= 1,75,200 BDT.

Table 7.1: Comparison of electricity generation for different choosing of module row spacing and corresponding electricity cost saving.

Percent-age of sunshine hour	Duration	Time span	Module Row Spacing from Sun-Path Diagram (mm)	Normal row spacing (mm)	Electricity generation of panel when normal row spacing is incorporated (KW-hour)	Electricity generation of panel when minimum row spacing from sun-path diagram is incorporated (KW-hour)	Cost of Electricity generation of panel when normal row spacing is incorporated (BDT)	Cost of Electricity generation of panel when minimum row spacing from sun-path diagram is incorporated (BDT)	Percentage cost saving
50%	6	9:00 AM – 3:00 PM	944.714	1385.2	1,75,200	2,10,240	8,76,000	10,51,200	16.67 %
55%	6.5	8:45 AM – 3:15 PM	1055.36			1,92,720		9,63,600	9.09 %
60%	7	8:30 AM – 3:30 PM	1201.52			1,75,200		8,76,000	0.00%
65%	7.5	8:15 AM – 3:45 PM	1289.21			1,75,200		8,76,000	0.00%
70%	8	8:00 AM – 4:00 PM	1417.25			1,75,200		8,76,000	0.00%

From the table we can see that, if we choose the minimum module row spacing at a percentage sunshine hour of 50% and a time span of 9:00 AM to 3:00 PM, then we can save the maximum money which is about 16.67 % of the cost of normal module row spacing.

7.1 Comparison Between Power Generation Per Unit Area And Thus Return Of More Money Throughout The Year By Using Conventional Module Row Spacing And Minimum Module Row Spacing Calculated From Our Model

7.1.1 Power generation per unit area by conventional module row spacing

= 175200/870 KW-hour per square meter.

= 201.38 KW-hour per square meter.

7.1.2 Return of money of power generation per unit are by conventional module row spacing

= 201.38×5.00 BDT.

= 1006.9 BDT.

7.1.3 Power generation per unit area by minimum module row spacing calculated from our model

= 2,10,240/870 KW-hour per square meter.

= 241.66 KW-hour per square meter.

7.1.4 Return of money of power generation per unit are by minimum module row spacing calculated form our model

= 241.66×5.00 BDT.

= 1208.28 BDT.

7.1.5 Percentage return of more money due to the use of minimum module row spacing

= 19.99 %

So from this calculation, we can see that, if we use the minimum module row spacing from out model we can generate almost 20% more money which is an amount of 201.38 BDT per square meter over the year.

CHAPTER 8

METHODOLOGY OF ANALYZING OF PARTIAL SHADING OF SURROUNDING OBJECTS FROM SUN-PATH DIAGRAM:

8. Methodology For Analyzing Of Partial Shading Of Surrounding Objects From Sun-Path Diagram

Despite advancements in photovoltaic technology, minor shading will still drastically reduce the performance of a solar cell module. Therefore, shade analysis should be performed before installation in order to assess the financial viability of an investment as well as to optimize the location and orientation of a photovoltaic cell.

As it is discussed earlier that a sun path diagram is essentially a plot of the sun's position, or path, in the sky at different times of the day and usually also for different months. The plot contains the solar altitude (the suns vertical position or elevation over the horizon) and the solar azimuth angle (the angle between the suns horizontal position and a reference direction, usually north or south).

Scanning the surrounding environment at the site of a PV system installation creates a horizon profile, showing the elevation of each surrounding object at its specific azimuth angle. Overlaying the horizon profile with the sun path diagram produces a shading diagram (Fig 8.1), where possible sources of near-object shading can easily be identified (UO Solar Radiation Monitoring Laboratory, 2008).

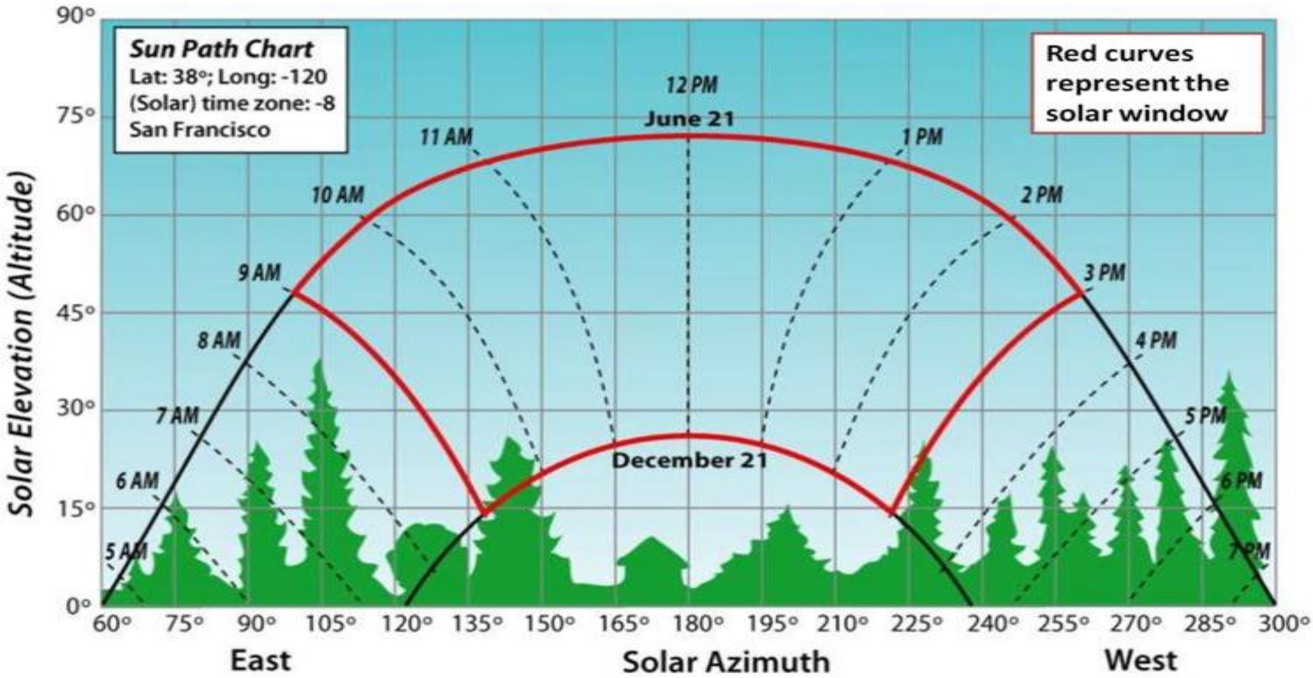

Fig 8.1: Shading diagram of solar elevation and azimuth of the sun together with the horizon outline of an object.

8.1 Instrument Used For Drawing Of Horizontal Profile On Sun-path Diagram

Fig – 8.2: Instruments used for drawing of horizon profile diagram on sun-path diagram.

In the fig-8.2, two instruments can be seen. One is the dome shaped sun-tracker, and another one is made in the Institute to finding out the solar elevation angle of the obstruction surrounding that space.

Now, the horizon profile which shows the elevation of each surrounding object at its specific azimuth angle is overlaid with the sun-path diagram. And it produces a shading diagram, where possible sources of near-object shading can easily be identified.

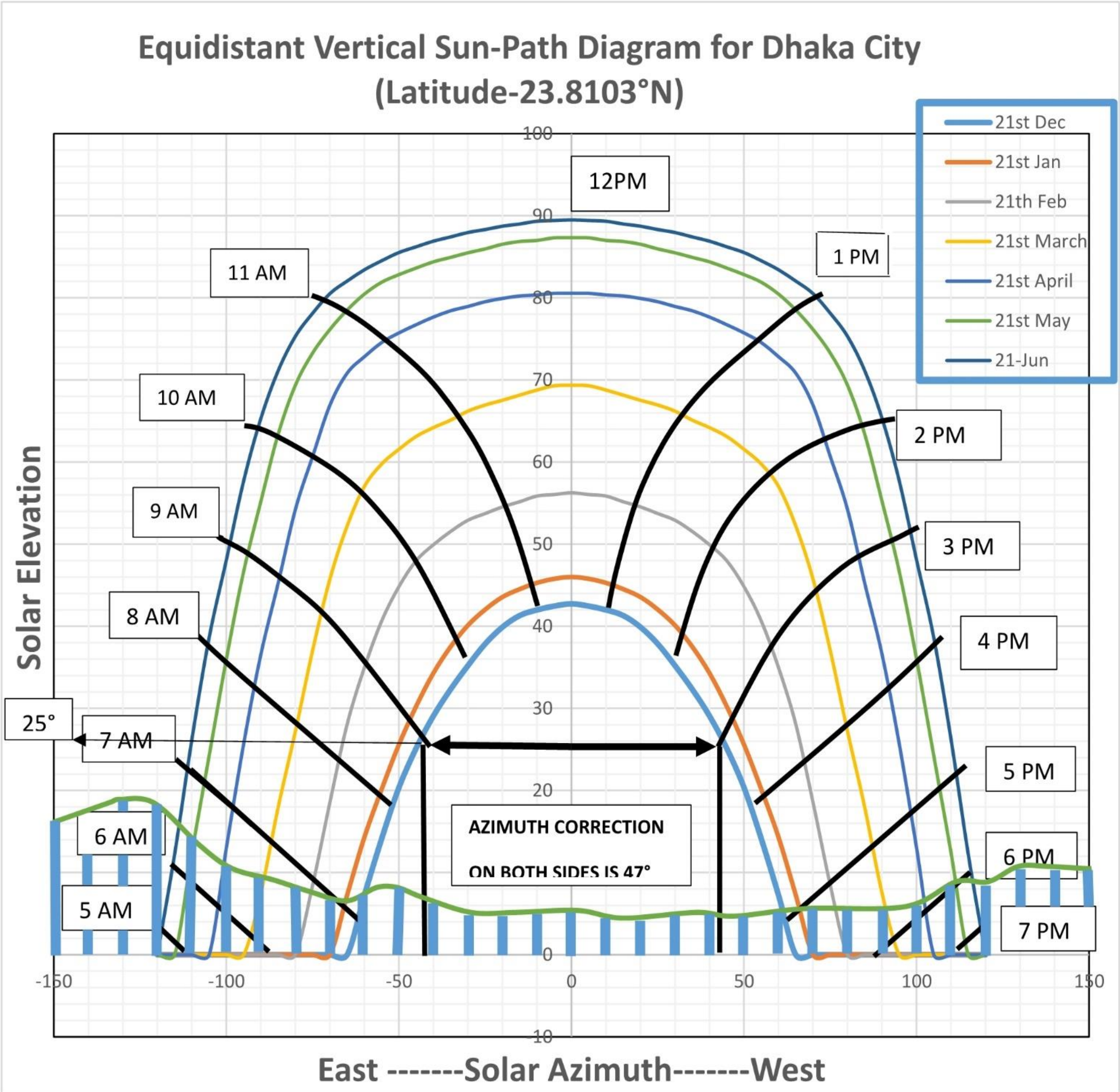

Fig 8.3: Shading diagram showing solar elevation and azimuth of the sun together with the horizon outline of an object.

From this figure, before even installation of the solar arrays, it can be analyzed that which obstacle may affect the solar panel. And the installer can decide which obstacles have to be removed and how much shading can be fall on the arrays at which part of the year. In this way, it can be a powerful tool of analysis for analyzing the shading effect even before the installation.

8.2 Calculation Of Percentage Decrease Of Diffuse Radiation From Sun-Path Diagram

Monthly average daily total irradiation on the tilted surface is

$$I(\beta) = I_{Bh}\cos\theta_i + I_D R_D + I_{Th} R_A$$ -------------9.2.1

Where:

I(β) = terrestrial insolation intensity on a plane tilted at β degrees to the horizontal surface (W/m^2);

I_{Bh} = terrestrial beam insolation intensity on a horizontal plane (W/m^2);

θ_i = angle of incidence of the radiation on the tilted plane;

I_D = diffused irradiation component on a horizontal plane (W/m^2);

R_D = a convention factor to adjust I_D to a value for a titled plane;

I_{Th} = the total terrestrial insolation intensity on a horizontal plane (W/m^2);

R_A = a convention factor used to find the reflected (or albedo) component for a titled plane. [24]

From equation 9.2.1, we can see that if the diffuse radiation is decreased so does the total irradiation.

From the sun-path diagram, by using the small square unit method, it is calculated that, almost 19.5% diffuse radiation will decrease from the solar panel established in front of the institute which will have a great impact on the total electricity generation by the plant.

So the site selection for this panel is not good enough for the optimal electricity generation. If it was set up on the rooftop, then we may increase the total electricity generation by the panel.

CHAPTER 9

CONCLUSION

9 CONCLUSION

This thesis studied about some specific fields. These are:

The minimum module row spacing of two adjacent rows of PV modules/panels in northern hemispheric geographical region from an organized mathematical model and all the calculation has performed based on information of Dhaka, Bangladesh. The minimum module row spacing is chosen for a sunshine hour of 50% and a time span of 6 hours from 9:00 AM to 3:00 PM is 934.894 mm for panels of width 1600 mm.

The minimum module row spacing of two adjacent rows of PV modules/panels in northern hemispheric geographical region from **SUN-PATH DIAGRAM** and all the calculation has performed based on information of Dhaka, Bangladesh.The minimum module row spacing is chosen for a sunshine hour of 50% and a time span of 6 hours from 9:00 AM to 3:00 PM is 944.714 mm for panels of width 1600 mm.

Comparative study of the value calculated from both the methods mentioned in (a) and (b).From this comparison, we can see that, there is only 1.05% deviation which is a pretty acceptable value.

Analysis of how more panels can be set up if the minimum module row spacing is incorporated and how much money can be saved. From this analysis, we can see that, for a space of length 30 m and width 29 m, 12 panels can be set up if minimum module row spacing of 944.714 mm where as only 10 panels can be set up if we choose the normal module row spacing. And throughout the year we can save 1,75,200 BDT. Over the year which is 16.67% of saving of money.

We have also calculated the power generation and return of money per square meter over the year by both conventional module row spacing as well as of module row spacing calculated from our model. We have calculated that we can generate 20% more money if we use the minimum module row spacing calculated form out mathematical model.

A shading diagram drawn by the overlaying of horizontal-profile over sun-path diagram which will provide information about which obstacles may cause shading at a specific time of day and year.We can analyze from the shading diagram that which obstacle may affect by shading at specific time over the year.

From the sun-path diagram, by using the small square unit method, it is calculated that, almost 19.5% diffuse radiation will decrease from the solar panel established in front of the institute which will have a great impact on the total electricity generation by the plant.

The mathematical model is solved by Matlab which is attached with this thesis book at the end.

9.2 FUTURE SCOPE OF THE WORK

1. The power generation is calculated by considering the efficiency of the solar panel as 20%. So power generation can be calculated by considering different panel materials and their corresponding efficiencies.

2. Again for different efficiencies, the saving of money can also be calculated and a comparative analysis can be done.

3. Due to time limitation the Matlab program used here is a segment-wise Matlab program. A complete one Matlab program can be done to reduce the consumption of time for calculation.

4. Different obstruction to solar panel has different porosity. And due to this variation of porosity, different amount of shading will be there on the panel. So analysis of porosity can give a better understanding of partial shading impact.

Bibliography

[1] "Ecotricity," 13 7 2016. [Online]. Available: https://www.ecotricity.co.uk/our-green-energy/energy-independence/the-end-of-fossil-fuels.

[2] O. Ellabban, H. Abu-Rub and F. Blaabjerg, "Ellabban, Omar; Abu-Rub, Haitham; Blaabjerg, Frede," *Renewable and Sustainable Energy Reviews,* pp. 748-764, 2013.

[3] H.-J. K. M. R. Sultan Ahmed Al Jaber, "Renewables 2010, Global Status Report," 2010.

[4] Y. Z. ,. I. G.-R. ,. R. H.-R. Ernesto Macías Galán, "RENEWABLES 2016," 2016.

[5] "www.irena.org," International Renewable Energy Agency, 2015. [Online]. Available: http://www.irena.org/menu/index.aspx?mnu=Subcat&PriMenuID=36&CatID=141&SubcatID=585. [Accessed 15 7 2016].

[6] "wikipedia," [Online]. Available: https://en.wikipedia.org/wiki/World_energy_consumption. [Accessed 10 8 2016].

[7] B. Kroposki, "Harnessing the Sun," *IEEE Power and Energy Magazine,* vol. 7(3), pp. 22-23, 2009.

[8] M. B. B. I. Gaetan Masson, "SNAPSHOT OF GLOBAL PHOTOVOLTAIC MARKETS," IEA-PVPS, 2015.

[9] F. W. Simon Wakter, "A novel shade analysis technique for solar photovoltaic systems," KTH School of Industrial Engineering and Management, STOCKHOLM, 2014.

[10] M. E. K. Y. W. W. &. d. Green, "Solar cell efficieny tables (version 41)," *Progress in Photovoltaics: Research and Applications.,* vol. 21(1).

[11] "PV-tec.org.," 2013. [Online]. Available: http://www.pv-tech.org/friday_focus/friday_focus_how_bangladesh_became_the_worlds_biggest_domestic_off_grid_pla. [Accessed 10 9 2016].

[12] T. &. O. T. Mishima, "A Power Compensation and Control System For a Partially Shaded PV Array.," *Electrical Engineerin in Japan.*

[13] D. Nnadi, "ENVIRONMENTAL/CLIMATIC EFFECT ON STAND-ALONE SOLAR ENERGY SUPPLY PERFORMANCE FOR SUSTAINABLE ENERGY," *Nigerian Journal of Technology (NIJOTECH),* Vols. Vol. 31, No. 1, 2012.

[14] D. S. a. U. S. R. E. Hanitsch, "Shading Effects on Output Power of Grid Connected Photovoltaic Generator Systems," *Rev. Energ. Ren: Power Engineering,* pp. 93-99, 2001.

[15] "www.volker-quaschning," 2003. [Online]. Available: http://www.volker-quaschning.de/articles/fundamentals1/index_e.php. [Accessed 15 6 2016].

[16] "NREL," [Online]. Available: http://www.nrel.gov/ncpv/. [Accessed 14 8 2016].

[17] "NASA Science Beta," 6 8 2008. [Online]. Available: https://science.nasa.gov/science-news/science-at-nasa/2002/solarcells/. [Accessed 23 8 2016].

[18] "Sargosis Solar & Electric PV Solar Specialists," [Online]. Available: http://sargosis.com/how-shade-affects-a-solar-array/. [Accessed 2 9 2016].

[19] R. &. V. J. Messenger, Photovoltaic systems engineering, 3rd edition, Boca Raton, Florida, 2010.

[20] C. L. P. Z. J. &. P. G. Chamberlin, "Effect of mismatch losses in photovoltaic arrays.," *Solar energy,* vol. 54, p. 3, 1995.

[21] B. A. C. &. R.-S. I. Galiana, "Explanation for the dark i-v curve of iii-v concentrator solar cells.," *Progress in Photovoltaics: Research and Applications ,* vol. 16, p. 4, 2008.

[22] J. &. M. C. Gow, "Development of a photovoltaic array model for use in power-electronics simulation study.," *IEE Proceedings - Electric Power Applications,* vol. 146, p. 2, 1999.

[23] A. &. H. S. Luque, Handbook of Photovoltaic Science and Engineering, Chichester, West Sussex, 2003.

[24] "ITCA," [Online]. Available: http://www.itacanet.org/the-sun-as-a-source-of-energy/part-4-irradiation-calculations/. [Accessed 2 9 2016].

Annexure-01

Segment-Wise Matlab Coding

```
%%%%% Finding out of shadow length of two consecutive parallel solar panels.
%%%%% Finding out of Value "B"
>> for n = 1:365
   B(n) = (360/364)*(n-81);
   end
>> B

%%%%% For each value of "B",  EoT (Equation of Time) is found out

>> EoT = 9.87*sin(2*B*(pi/180)) - 7.53*cos(B*(pi/180)) - 1.5*sin(B*(pi/180))

    EoT=

%%%%% Value of LSTM (Local standard time meridian) = 90°

%%%%% Finding out of TC (Time Correction) for all Equation of Time

>> TC = 4*(90-90.4125) + E

    TC =

%%%%% Finding out of LST(Local Solar Time in hours) from LT(Local Time) and TC(Time Correction)

>> LST = LT + (TC/60)

%%%%% Finding out of Hour angle for LST (Local Standard Time)

>> O = 15*(S-12)

%%%%% Finding out of declination angle over the year

for n = 1:365

 D (n) = 23.45*sin(360*(pi/180)*((284+n)/365));

 end

>> D

    D =

%%%%% Finding out of solar altitude angle

>> A = [(asin(sin(23.8103*(pi/180))*sin(-23.0116*(pi/180)) + cos(23.8103*(pi/180))*cos(
               23.0116*(pi/180))*cos(O*(pi/180)))) * (180/pi)]

    A =

%%%%%Finding out of azimuth angle

 >> B = [(acos(((sin(25.0758*(pi/180)))*(sin(23.8103*(pi/180))) - (sin(-
 23.0116*(pi/180))))/((cos(25.0758*(pi/180)))*(cos(23.8103*(pi/180))))))*180/pi];

    B=
```

```
>>Shadow length = w*cos(23.8103*pi/180)  +   w*sin(23.8103*pi/180)*(((cos B)*(pi/180))/((tan A)*(pi/180)))
Shadow length =
```
